Recombinant Acid Ceramidase Reduces Inflammation and Infection in Cystic Fibrosis

Aaron I. Gardner[1], Iram J. Haq[1,2], A. John Simpson[1,3], Katrin A. Becker[4], John Gallagher[1], Vinciane Saint-Criq[5], Bernard Verdon[5], Emily Mavin[1], Alexandra Trigg[1], Michael A. Gray[5], Albert Koulman[6], Melissa J. McDonnell[5,7], Andrew J. Fisher[1], Elizabeth L. Kramer[8,9], John P. Clancy[8,9], Christopher Ward[1], Edward H. Schuchman[10], Erich Gulbins[4,11] and Malcolm Brodlie*[1,2]

[1]Translational and Clinical Research Institute, Faculty of Medical Sciences, Newcastle University, Newcastle upon Tyne, UK.

[2]Paediatric Respiratory Medicine, Great North Children's Hospital, Newcastle upon Tyne Hospitals NHS Foundation Trust, Newcastle upon Tyne, UK.

[3]Respiratory Medicine, Freeman Hospital, Newcastle Upon Tyne Hospitals NHS Foundation Trust, Newcastle Upon Tyne, UK

[4]Department of Molecular Biology, University of Duisburg-Essen, Essen, Germany.

[5]Biosciences Institute, Faculty of Medical Sciences, Newcastle University, Newcastle upon Tyne, UK.

[6]NIHR BRC Metabolomics and Lipidomics Facility, University of Cambridge, Cambridge, UK.

[7]Department of Respiratory Medicine, Galway University Hospital, Galway, Ireland.

[8]Department of Pediatrics, Cincinnati Children's Hospital Medical Centre, Cincinnati, USA.

[9]Division of Pulmonary Medicine, Cincinnati Children's Hospital Medical Centre, Cincinnati, USA.

[10]Department of Genetics & Genomic Sciences, Icahn School of Medicine at Mount Sinai, New York, USA.

[11]Department of Surgery, University of Cincinnati, Cincinnati, USA.

*To whom correspondence should be addressed: Malcolm Brodlie, MRC Clinician Scientist/Honorary Consultant in Paediatric Respiratory Medicine, Level 3, Clinical Resource Building, Great North Children's Hospital, Queen Victoria Road, Newcastle upon Tyne, UK, NE1 4LP. E-mail: malcolm.brodlie@ncl.ac.uk. Tel: +44 191 2336161.

Author contributions

AG: Performed experiments, analyzed data and wrote the first draft of the manuscript. IH, KAB, JG, VS-C, BV, EM, AT, MAG, AK, MJM, AJF, ELK and JPC: Contributed to experiments, commented on the manuscript. CW, AJS, EHS and EG: Involved in conception of the study, performed experiments and commented on the manuscript. MB: Conceived the study, analyzed data and wrote the final version of the manuscript.

Sources of support

Running head

Acid ceramidase, inflammation and infection in CF

Descriptor

9.17 Cystic Fibrosis: Translational & Clinical Studies

Total word count

3,831

Online Data Supplement statement - This article has an online data supplement, which is accessible from this issue's table of content online at www.atsjournals.org

Impact of this research

We demonstrate that the sphingolipid profile in cystic fibrosis (CF) airway epithelial cells is abnormal due to altered function of metabolizing enzymes leading to ceramide accumulation and a lack of upregulation of sphingosine, which has antimicrobial properties, in response to *Pseudomonas aeruginosa*. It is possible to modulate ceramide levels via treatment with recombinant acid ceramidase and demonstrate reduced susceptibility to infection and inflammation. Acid ceramidase is already being used therapeutically in people with Farber Disease and therefore has translational potential to be repurposed to ameliorate the two pivotal features of cystic fibrosis lung disease, inflammation and infection.

At a Glance Commentary

Scientific Knowledge on the Subject:

Cystic fibrosis lung disease is characterised by inflammation and susceptibility to infection. The pathogenesis of cystic fibrosis lung disease is not fully elucidated and both of these processes remain problems in people with cystic fibrosis receiving modulator therapies. Sphingolipids form specialized membrane domains that modulate a diverse range of biological processes. Increased levels of the sphingolipid ceramide have been reported in the airway epithelium of cystic fibrosis murine models that when normalized reduced inflammation and susceptibility to the key pathogen *Pseudomonas aeruginosa*. Studies using human model systems are lacking, representing an important gap.

What This Study Adds to the Field:

Here, we show using differentiated cultures of airway epithelial cells from people with cystic fibrosis combined with mass spectrometry that ceramide is increased due to differential expression and function of metabolizing enzymes. Furthermore, cystic fibrosis epithelial cells do not upregulate sphingosine, a metabolite of ceramide with anti-microbial properties, in response to *P. aeruginosa* infection. Treatment with recombinant acid ceramidase decreased ceramide levels and reduced inflammatory mediator production and susceptibility to infection in cystic fibrosis epithelial cell cultures and lung inflammation in murine models. These findings suggest a novel therapeutic approach worthy of further exploration.

Abstract

Rationale: In cystic fibrosis the major cause of morbidity and mortality is lung disease characterized by inflammation and infection. The influence of sphingolipid metabolism is poorly understood with a lack of studies using human airway model systems.

Objectives: To investigate sphingolipid metabolism in cystic fibrosis and the effects of treatment with recombinant human acid ceramidase on inflammation and infection.

Methods: Sphingolipids were measured using mass spectrometry in fully-differentiated cultures of primary human airway epithelial cells and co-cultures with *Pseudomonas aeruginosa*. *In situ* activity assays, Western blotting and quantitative polymerase chain reaction were used to investigate function and expression of ceramidase and sphingomyelinase. Effects of treatment with recombinant human acid ceramidase on sphingolipid profile and inflammatory mediator production were assessed in cell cultures and murine models.

Measurements and Main Results: Ceramide is increased in cystic fibrosis airway epithelium due to differential function of enzymes regulating sphingolipid metabolism. Sphingosine, a metabolite of ceramide with antimicrobial properties, is not upregulated in response to *Pseudomonas aeruginosa* by cystic fibrosis airway epithelia. Tumor necrosis factor receptor 1 is increased in cystic fibrosis epithelia and activates NF-κB signaling, generating inflammation. Treatment with recombinant human acid ceramidase, to decrease ceramide, reduced both inflammatory mediator production and susceptibility to infection.

Conclusions: Sphingolipid metabolism is altered in airway epithelial cells cultured from people with cystic fibrosis. Treatment with recombinant acid ceramidase

ameliorates the two pivotal features of cystic fibrosis lung disease, inflammation and infection, and thus represents a therapeutic approach worthy of further exploration.

[Word count 248]

Key words

sphingolipid; ceramide; sphingosine; lung

Introduction

Cystic fibrosis (CF) is among the most common life-limiting genetic disorders worldwide(1, 2). The major cause of morbidity and mortality in CF is lung disease characterized by neutrophilic inflammation, mucus retention and susceptibility to endobronchial infection with, in particular, *Staphylococcus aureus* and *Pseudomonas aeruginosa*(1). A cycle of inflammation and infection ensues, resulting in progressive bronchiectasis. Several hypotheses have been proposed to explain the pathophysiology seen in CF lung disease, including abnormal volume, pH and electrolyte content of the airway surface liquid(3-8). However, the precise mechanisms are not fully elucidated and multiple processes that impact on inflammation and defense against infection are likely to be involved.

Sphingolipids form membrane domains that can interact to alter the function of membrane components and modulate a diverse range of biologically important processes(9). Sphingolipids have previously been linked to CF pathophysiology. Increased levels of ceramide have been identified in the airway epithelium of CF murine models that, when normalized, reduced inflammation and susceptibility to *P. aeruginosa* infection(10, 11). Raised ceramide has also been found in the epithelium of lungs removed at the time of transplantation from people with CF(12). Reports have suggested that relative concentrations of ceramides may be important, with different chain lengths over- and under-represented in the blood of people with CF and murine models(13-15). Lipidomic analysis of bronchoalveolar lavage (BAL) fluid has recently demonstrated an altered profile in CF(16, 17).

Studies using human airway model systems are lacking, representing an important gap. In part, this is due to the fact that fully differentiated cultures of primary human bronchial airway epithelial cells from people with CF present technical challenges (18). In the context of sphingolipid metabolism, this human model allows investigation of underlying mechanisms and refinement of targets for intervention.

Here we investigate the metabolism of ceramides using primary human airway epithelial cell cultures, BAL fluid and murine models. We describe how the function of key enzymes involved in ceramide metabolism - acid sphingomyelinase (which converts sphingomyelin to ceramide) and acid ceramidase (which converts ceramide to sphingosine) - is altered in CF. This promotes accumulation of ceramides that in turn leads to inflammation (generated via tumor necrosis factor receptor 1 (TNFR1) activation and NF-κB signaling), and susceptibility to infection (due to lack of upregulation of sphingosine). Treatment of airway epithelial cell cultures with recombinant human acid ceramidase (rhAC) decreased inflammation and infection. Furthermore, in murine models, nebulization of rhAC reduced airway inflammation, suggesting a therapeutic approach worthy of further investigation.

Methods

Primary airway epithelial cell culture and culture treatment

Primary bronchial epithelial cells were cultured at an air liquid interface (ALI) as previously described(18). Clinical characteristics of the patients studied are in Table E1 in the online data supplement. All cultures generated cilia, produced mucus and had a trans-epithelial resistance >250 Ω*cm^2.

For co-culture experiments ALI cultures were transitioned to antibiotic-free medium, and 1×10^5 colony forming units of *P. aeruginosa* (PA01) in 100 μL phosphate-buffered saline were added to the apical surface, and incubated for 24 hours. In specific experiments, cultures were treated apically for 1 hour with: 100 μL of rhAC (20 μg/mL), generated as described previously[19]; the highly selective and potent cRel inhibitor IT 901 (2 μM) for 24 hours; or the CF transmembrane conductance regulator (CFTR) modulators ivacaftor or tezacaftor-ivacaftor in combination (each 5 μM) for 48 hours with dose refreshed after 24 hours.

Detailed methods, including sample preparation for analysis, and standard methodologies (Western blotting, real-time qPCR and ELISA) are provided in the online data supplement.

Analysis of sphingolipid profile of cell cultures by mass spectrometry

Calibration curves for all assayed ceramide and sphingosine species were constructed using appropriate standards. All standards and samples were analyzed in triplicate with the ABSciex QTrap 4000 system, using a 3-scan event methodology to reduce matrix noise. For selectivity the mass tolerance for each ion was set to within 0.01 m/z, which allowed for accurate quantification.

BAL ceramide measurement

For ceramide determination, a ceramide hydrolysis buffer (0.2 M citric/phosphate buffer, 0.3 M NaCl and 0.2 mg/ml of recombinant acid ceramidase) was mixed with the total lipid extract solution (1:1,v/v) and incubated at 37 °C for 1 hour. Cell-free

supernatant samples were analyzed using an Acquity H-Class UPLC system equipped with a Waters Acquity UPLC BEH RP18 column.

Ceramidase and sphingomyelinase functional *in situ* assays

100 µL of buffered solution containing either BODIPY® TR Ceramide or BODIPY® FL C12-Sphingomyelin at a 1:2000 dilution was applied to the apical surface of ALI cultures. The lipid fraction was isolated as described in the online data supplement and samples were separated by thin layer chromatography with chloroform:methanol (5:1 v/v).

Mice studies

Two different *Cftr* mutant mouse strains and their respective syngeneic littermates were used. *Cftr*^{tm1Unc}-*Tg*$^{(FABPCFTR)}$ (abbreviated *Cftr*^{KO}) Jaw mice are genetically deficient for the murine equivalent to human CFTR (*Cftr*), but express human CFTR in the gut under control of a fatty acid binding protein promoter to prevent acute intestinal obstruction. B6.129P2(CF/3)-*Cftr*$^{TgH(neoim)Hgu}$ (abbreviated *Cftr*^{MHH}) congenic mice were also used that have a low residual activity of Cftr allowing normal development and feeding.

Nebulization of recombinant human acid ceramidase

Cftr^{KO} and *Cftr*^{MHH} mice were nebulized with rhAC 200 µg diluted in 800 µL 0.9% NaCl solution using Pari boy nebulizer apparatus over 10 minutes. rhAC was nebulized on 3 consecutive days when mice were 24 weeks old. The trachea was removed 6 hours after the last inhalation for further analysis as described in the online data supplement.

Results

Ceramide metabolism is dysregulated in cystic fibrosis airway epithelial cells

Mass spectrometry was used to investigate the ceramide profile in primary bronchial epithelial cells isolated from people with CF or controls, and fully differentiated at an ALI. Clinical characteristics of the patients studied are in Table E1 in the online data supplement. Under basal conditions, total levels of ceramide were increased in CF cultures (Fig 1a) with similar levels of sphingosine, a key metabolite of ceramide, in CF and non-CF cultures (Fig 1b). There was increased C16 and C22 ceramide in CF cultures (Fig 1c). In murine models, normalization of sphingolipids has been associated with reduction in susceptibility to *P. aeruginosa,* the most significant respiratory pathogen in CF(10)*.* We therefore investigated the ceramide profile of cultures following co-culture with live *P. aeruginosa.* In both CF and non-CF cultures total ceramide was increased following exposure to *P. aeruginosa* (Fig 1a), with statistically significant increases in C16, C20 and C22 observed in CF cultures only (Fig 1c). An increase in sphingosine occurred in non-CF cultures exposed to *P. aeruginosa* (Fig 1b). However, in CF cultures *P. aeruginosa* did not induce changes. Sphingolipids are pivotal constituents of plasma membranes with enriched domains crucial for modulating cellular functions. We therefore also measured sphingolipid concentrations in plasma membrane fractions and found a similar pattern to that in whole cell lysates for ceramide and sphingosine (Figs 1d-f). The proportion of ceramide in membrane fractions was comparable across all experiments (Fig 1g). An increase in sphingosine occurred in non-CF cultures exposed to *P. aeruginosa* in plasma membrane fractions (Fig 1e) with an increase in percentage present in the

plasma membrane (Fig 1h). Similar to results in whole cell lysates, *P. aeruginosa* did not induce changes in plasma membrane sphingosine in CF cultures (Figs 1e and 1h).

Collectively, these data suggest that ceramide accumulates in human CF airway epithelial cells with a distinct profile of individual species present, including both long chain and very long chain ceramides. In response to *P. aeruginosa* non-CF cultures upregulate sphingosine, an effect not seen in CF cultures.

Ceramide is increased in BAL fluid from children and young people with cystic fibrosis

To test whether the situation *in vitro* was mirrored *in situ*, we measured total ceramide in BAL fluid collected during clinically-indicated bronchoscopies from children and young people with CF and an age-matched comparator group who do not have CF but underwent investigation for respiratory problems (clinical details are in Table E1 in the online data supplement). Levels of ceramide were increased in the CF group (Fig 2a).

In cystic fibrosis epithelia there is decreased function of ceramidase and increased function of sphingomyelinase

To investigate potential mechanisms responsible for ceramide accumulation we measured functional enzyme activity at the apical surface of cell cultures. Total ceramidase activity was reduced in CF cultures (Fig 3a). Acid ceramidase protein and *ASAH1* (coding for acid ceramidase) gene expression were decreased in CF cells compared to non-CF (Figs 3b and c). Following co-culture with *P. aeruginosa* there was an increase in acid ceramidase protein and *ASAH1* gene expression in non-CF cultures with a smaller increase observed in CF cultures (Figs 3b and c).

Conversely, sphingomyelinase activity was increased (Fig 3d) in CF cultures. However, there was no difference in acid sphingomyelinase protein or the expression of the *SMPD1* (coding for acid sphingomyelinase) gene between any cell type or treatment (Figs 3e and f).

Together, these data suggest that a combination of reductions in expression and function of acid ceramidase (which converts ceramide to sphingosine) and an increase in sphingomyelinase (which converts sphingomyelin to ceramide) function serve to promote the accumulation of ceramide observed in human CF airway epithelium.

Treatment with recombinant human acid ceramidase reduces levels of ceramide in cystic fibrosis airway epithelia

Based on Figure 3, we assessed the capacity for rhAC to modulate ceramide levels in human airway epithelial cells. rhAC has recently been developed as an enzyme replacement therapy for Farber disease[20-22]. Initial experiments established no cytotoxic effect of rhAC on airway epithelial cell cultures (Figs E2a and b in the online data supplement). A single treatment of CF cultures with rhAC reduced ceramide and restored levels close to those seen in non-CF cultures (Fig 4a). For sphingosine, no statistically significant differences were detected at the whole cell level (Fig 4b). Treatment with rhAC reduced C16, C22 and C24 ceramide (Fig 4c). In plasma membrane fractions, a similar reduction in total ceramide was observed (Fig 4d) along with an increase in sphingosine levels (Fig 4e) that was statistically significant in non-CF cultures. At the individual species level, only C24 ceramide was statistically significantly reduced (Fig 4f). Following rhAC treatment the proportion of ceramide in the plasma membrane was unchanged (Fig 4g) and the proportion of sphingosine

present in the plasma membrane in both CF and non-CF cultures was increased (Fig 4h).

Inflammatory responses are reduced following treatment with recombinant human acid ceramidase

Neutrophilic airway inflammation is a pivotal part of CF lung disease pathophysiology(1). In view of the role of sphingolipids in modulating inflammatory responses we investigated the effect of rhAC treatment on inflammatory mediator production at the apical surface of airway epithelial cell cultures(9). At baseline, increased secretion of IL-8, IL-1β and TNFα (Figs 5a-c), was observed in CF cultures, with no statistically significant differences seen in IL-4 or IL-6, (Figs E3a-b in the online data supplement). Application of rhAC resulted in significantly reduced secretion of IL-8 in CF cultures, to levels comparable with control non-CF cultures, and this effect was maintained for 5 days following a single treatment (Fig 5a). A similar, though less marked, effect of rhAC was observed for IL-1β, TNFα (Figs 5b and c) and IL-6 (Fig E3a in the online data supplement). Comparison was made with the effect of modulating CFTR function in CF cultures homozygous for F508del with ivacaftor or tezacaftor-ivacaftor. Again, treatment with rhAC reduced IL-8 production with a small, but not statistically significant, reduction seen with tezacaftor-ivacaftor and no synergistic effect with rhAC and tezacaftor-ivacftor (Fig 5d).

To further investigate the potential for rhAC as an anti-inflammatory therapy in CF, we examined the effect of nebulized rhAC on airway inflammation in two different CF murine models. *Cftr*^{tm1Unc}*-Tg*^(FABPCFTR) (*Cftr*^{KO}) mice are genetically deficient for the murine equivalent to human CFTR (Cftr), but express human CFTR in the gut under control of a fatty acid binding protein promoter to prevent acute intestinal obstruction.

In contrast, B6.129P2(CF/3)-*Cftr*$^{TgH(neoim)Hgu}$ (*Cftr*^{MHH}) congenic mice have a low residual activity of Cftr allowing normal development and feeding. Increased numbers of neutrophils and macrophages were observed in the lungs of CF mice (Figs 6a and b). This was associated with increased ceramide levels (Fig E4a in the online data supplement). Nebulization of rhAC to mice daily for 3 days reduced neutrophil and macrophage numbers towards wild type levels (Figs 6a and b).

These data suggest that treatment with rhAC reduces the production of several key pro-inflammatory cytokines and chemokines by CF airway epithelial cell cultures. Furthermore, nebulization of rhAC in two different murine models was associated with a reduction in cellular markers of lung inflammation.

Inflammatory responses are driven by altered tumor necrosis factor receptor 1 expression and NF-κB activation

Changes in the lipid composition of plasma membranes can significantly alter receptor expression and downstream signaling events(11, 23). Sphingolipid-enriched membrane domains have been shown to be essential for TNFR1 activation and subsequent NF-κB signaling(24). We investigated TNFR1 expression in CF cultures and found it to be increased compared to non-CF cultures (Figs 7a and b). This reduced following treatment with rhAC (Figs 7a and b). These findings were confirmed by Western blotting for TNFR1 in plasma membrane fractions (Fig E5 in the online data supplement). To investigate downstream signaling from TNFR1 we investigated expression and nuclear localization of NF-κB subunit cRel (Figs 7c and d). Co-culture with *P. aeruginosa* resulted in an increase in the nuclear localization of cRel in CF cultures. Treatment with rhAC increased cytoplasmic cRel, with a corresponding reduction in nuclear localization of cRel (Figs 7c and d). Use of a specific cRel inhibitor

reduced IL-8 production (Fig 7e). In human airway tissue sections (clinical details are shown in Table E1 in the online data supplement), significantly more cRel was localized in the nucleus of epithelial cells from people with advanced CF lung disease compared to unused donor lungs (Figs 7f-h). Due to TNFR1 also being expressed at the basolateral membrane of airway epithelial cells we measured TNFα in the basolateral medium in the experiments shown in Fig 5c. Levels of TNFα were higher in the basolateral medium than in the apical washes (Fig E3c).

These data suggest that CF epithelia have increased TNFR1 expression that reduces following treatment with rhAC and the decrease in ceramide levels. Consequently, enhanced NF-κB activation is observed in CF epithelia with increased nuclear localization of cRel, which also reduces with rhAC treatment.

Treatment with recombinant human acid ceramidase reduces susceptibility to infection

Previous work has shown that reduction of ceramide in the airways of CF mice is associated with a reduction in susceptibility to infection(10, 11). We therefore examined effects of rhAC treatment on infection in primary human airway epithelial cells using two different methods.

Firstly, heat-killed, fluorescently labeled *S. aureus* were added to the apical surface of differentiated cultures. Increased numbers of *S. aureus* remained adherent to the surface of CF cultures, suggestive of an increased susceptibility to colonization (Figs 8a and b). Treatment with rhAC reduced the adherence of *S. aureus* to CF cultures (Figs 8a and b).

Secondly, we investigated defense against live *P. aeruginosa.* Increased viable bacteria were isolated from the surface and lysates of CF cultures (Figs 8c and d). Treatment with rhAC reduced the number of viable *P. aeruginosa* recovered from the apical surface of cultures (Fig 8c), while no significant reduction in bacteria internalized by CF cultures was observed (Fig 8d).

Discussion

Through mass spectrometry analysis of differentiated primary airway epithelial cell cultures we have shown, and quantified, an altered ceramide profile in human CF epithelia. Increased ceramide was also detected in BAL fluid from children and young people with CF. This supports previous observations made in some murine models and agrees with immunohistochemistry performed on the bronchial epithelium of explanted advanced CF lung disease tissue (10, 12, 13).

Previous studies of sphingolipids in CF, using different models and techniques, have found varying results(15). In homogenized explanted lung tissue (containing multiple cell types and representing end-stage disease) increased C16, C18 and C20, but not C22, ceramide species were observed(12). In contrast, a cell line model transfected with an antisense *CFTR* construct demonstrated reduced levels of C18, but increased levels of C22, C24 and C26(25). Findings in another CF murine model and the peripheral blood of people with CF have suggested a reduction in C24 ceramide and increase in C16(13, 15). Here, using a fully differentiated model in primary human epithelial cells we found increased C16 and C22 in whole cell lysates and increased C24 in the plasma membrane. These ceramide chain lengths and their metabolites are known to be involved in inflammation and apoptosis(9, 12, 15, 26-31).

Data presented here suggest that ceramide accumulates in CF airway epithelia due to differential function of enzymes. Decreased ceramidase function combined with increased sphingomyelinase activity favor increased ceramide accumulation. Western blot and gene expression analysis further showed that the decreased ceramidase activity was due to reduced acid ceramidase expression. This agrees with work in CF murine models showing that β1-integrin is trapped in the apical membrane of airway epithelial cells, downregulating acid ceramidase expression(11).

In the case of acid sphingomyelinase we found expression to be unchanged in CF epithelia. The reason for the altered activity of acid sphingomyelinase remains uncertain. Under *in vitro* conditions acid sphingomyelinase is a much more active enzyme than acid ceramidase (i.e., has a 10-fold or greater capacity to hydrolyze sphingomyelin compared with the ability of acid ceramidase to hydrolyze ceramide)(32). One possible explanation for reduced activity is that acid sphingomyelinase function is known to be pH dependent (activity increases as pH lowers to an optimum of around 5)(33, 34). The pH of the airway surface liquid in CF remains keenly debated, however, there is some evidence to suggest that homeostasis is disordered and that the pH is lowered(3, 4, 35-38). Another potential explanation, is that acid ceramidase and acid sphingomyelinase are known to exist in a complex with inter-connected functions(19). It is therefore possible that reduced acid ceramidase expression may lead to a conformational change in acid sphingomyelinase and further enhanced enzyme activity.

Treatment of CF cultures with rhAC decreased ceramide close to levels present in non-CF cultures and reduced secretion of inflammatory mediators. Nebulization of rhAC in CF mouse models also reduced lung inflammation. We found evidence of

neutrophilic inflammation in the lungs of *Cftr^KO* and *Cftr^MHH* mice. A constitutive increase in expression of IL-1 and the mouse homolog of IL-8, keratinocyte-derived chemokine, has been shown in lung homogenates from these mice (10). Reduction of ceramide levels (genetically by crossing with acid sphingomyelinase knock out animals or pharmacologically via amitriptyline treatment) has also been shown to lead to a reduction in neutrophilic inflammation(10). Our work would have been strengthened by measurement of key cytokines and chemokines in the murine lung, histological assessment of neutrophil and macrophage distribution, and by studying *in vivo* responses to airway infection.

There are divergent findings in the literature around the existence of a pro-inflammatory state in the CF airway in the absence of identifiable infection, with some evidence to support this concept from BAL studies in young children but varied findings in other studies and animal models(1, 39-44). In our primary human airway epithelial model we found increased production of several pro-inflammatory mediators in cultures derived from adults with advanced CF lung disease. The effects of altered membrane microdomain abundance on relative fluidity and stability of transmembrane receptors involved in inflammatory responses and activity of ion channels remains poorly understood(15, 45, 46). Notably, Abu-Arish *et al.* recently demonstrated that epithelial cells respond to secretagogues by forming clusters of CFTR in ceramide-rich membrane microdomains via an acid sphingomyelinase-dependent mechanism to increase transepithelial secretion(47). We found that reducing ceramide in CF epithelial cells, via rhAC treatment, was associated with reduced TNFR1 expression, decreased cRel nuclear localization and less IL-8 production. It is recognized that activation of NF-κB results in IL-8 production, however, epigenetic factors and mRNA

stability also influence this process and how a change in sphingolipid profile impacts on these is yet to be elucidated (48-50).

Relatively low levels of TNFα, in the range of 1-2 pg/mL in apical washings and 5-9 pg/mL in basolateral medium, were measured in unstimulated cultures, in keeping with those reported in the literature (51). However, epithelial cells are not the only source of TNFα in the CF lung, with reports of production by macrophages and neutrophils (52). Several studies have measured levels of TNFα in airway samples from people with CF. For example, mean levels of 130 and 400 pg/mL have been measured in sputum and BAL fluid respectively, with higher concentrations during pulmonary exacerbations(52-54).

We also found increased susceptibility to infection in CF cultures that was reduced by rhAC treatment. Sphingosine, which is generated from ceramide by acid ceramidase, is known to have antimicrobial properties and has been found to be deficient in the airway of CF murine models(11). We did not detect differences in sphingosine between CF and non-CF human cultures at baseline. However, unlike non-CF cells, on exposure to *P. aeruginosa* CF epithelial cells did not upregulate levels of sphingosine in the plasma membrane. We propose that this represents a potentially important host-defense mechanism, dysfunction of which may contribute to the susceptibility to respiratory infection seen clinically in people with CF. Treatment with rhAC did increase plasma membrane sphingosine in cell cultures but this effect was only statistically significant in non-CF cultures. A potential explanation for this is that sphingosine produced following rhAC treatment may be rapidly metabolized. In a mouse model of Farber disease intraperitoneal rhAC treatment markedly reduced ceramide levels but sphingosine increased to a lesser extent, especially so in the lung

compartment(22). When considering the proportion of sphingosine in the plasma membrane there was a significant increase in both CF and non-CF cultures with rhAC treatment. This localized increase in sphingosine may account for the effect of rhAC treatment on reducing bacterial adherence to the apical plasma membrane, but not internalization.

Limitations of our infection work are that we used a laboratory strain of *P. aeruginosa* rather than a clinical isolate and did not work with live *S. aureus.* Proof of principle data were generated to investigate the effects of acute rhAC treatment on inflammation and infection. To advance along a translational path further evidence will likely need to be generated for longer-term treatment and efficacy in larger animal models prior to experimental medicine studies in humans.

Collectively, our work supports the concept that disordered sphingolipid metabolism is involved in CF lung disease pathogenesis - linking to both inflammation and infection. Our proposed model is summarized in Figure 9. Restoring acid ceramidase activity with rhAC treatment therefore represents an intriguing novel potential approach to target these two key pathological processes in the airways of people with CF. Despite exciting developments in the field of CFTR modulators there remains an unmet need to develop therapies that ameliorate ongoing problems with inflammation and infection(55). It is also unlikely that any single medication will fully treat the complex pathophysiology of CF lung disease and highly probable that people with CF will continue to be treated with a combination of drugs in the future. The fact that rhAC is currently being developed as a treatment for patients with Farber disease highlights the potential of re-purposing this drug for CF(56, 57). Towards this end, we have

demonstrated that rhAC may be delivered in nebulized form to mice and has important effects *in vivo*.

Acknowledgements

References

1. Elborn JS. Cystic fibrosis. *Lancet* 2016; 388: 2519-2531.

2. Ramsey BW, Downey GP, Goss CH. Update in Cystic Fibrosis 2018. *Am J Respir Crit Care Med* 2019; 199: 1188-1194.

3. Haq IJ, Gray MA, Garnett JP, Ward C, Brodlie M. Airway surface liquid homeostasis in cystic fibrosis: pathophysiology and therapeutic targets. *Thorax* 2016; 71: 284-287.

4. Pezzulo AA, Tang XX, Hoegger MJ, Abou Alaiwa MH, Ramachandran S, Moninger TO, Karp PH, Wohlford-Lenane CL, Haagsman HP, van Eijk M, Banfi B, Horswill AR, Stoltz DA, McCray PB, Jr., Welsh MJ, Zabner J. Reduced airway surface pH impairs bacterial killing in the porcine cystic fibrosis lung. *Nature* 2012; 487: 109-113.

5. Hoegger MJ, Fischer AJ, McMenimen JD, Ostedgaard LS, Tucker AJ, Awadalla MA, Moninger TO, Michalski AS, Hoffman EA, Zabner J, Stoltz DA, Welsh MJ. Impaired mucus detachment disrupts mucociliary transport in a piglet model of cystic fibrosis. *Science* 2014; 345: 818-822.

6. Tang XX, Ostedgaard LS, Hoegger MJ, Moninger TO, Karp PH, McMenimen JD, Choudhury B, Varki A, Stoltz DA, Welsh MJ. Acidic pH increases airway surface liquid viscosity in cystic fibrosis. *J Clin Invest* 2016; 126: 879-891.

7. Garland AL, Walton WG, Coakley RD, Tan CD, Gilmore RC, Hobbs CA, Tripathy A, Clunes LA, Bencharit S, Stutts MJ, Betts L, Redinbo MR, Tarran R. Molecular

basis for pH-dependent mucosal dehydration in cystic fibrosis airways. *Proc Natl Acad Sci U S A* 2013; 110: 15973-15978.

8. Matsui H, Grubb BR, Tarran R, Randell SH, Gatzy JT, Davis CW, Boucher RC. Evidence for periciliary liquid layer depletion, not abnormal ion composition, in the pathogenesis of cystic fibrosis airways disease. *Cell* 1998; 95: 1005-1015.

9. Maceyka M, Spiegel S. Sphingolipid metabolites in inflammatory disease. *Nature* 2014; 510: 58-67.

10. Teichgraber V, Ulrich M, Endlich N, Riethmuller J, Wilker B, De Oliveira-Munding CC, van Heeckeren AM, Barr ML, von Kurthy G, Schmid KW, Weller M, Tummler B, Lang F, Grassme H, Doring G, Gulbins E. Ceramide accumulation mediates inflammation, cell death and infection susceptibility in cystic fibrosis. *Nat Med* 2008; 14: 382-391.

11. Grassme H, Henry B, Ziobro R, Becker KA, Riethmuller J, Gardner A, Seitz AP, Steinmann J, Lang S, Ward C, Schuchman EH, Caldwell CC, Kamler M, Edwards MJ, Brodlie M, Gulbins E. beta1-Integrin Accumulates in Cystic Fibrosis Luminal Airway Epithelial Membranes and Decreases Sphingosine, Promoting Bacterial Infections. *Cell Host Microbe* 2017; 21: 707-718 e708.

12. Brodlie M, McKean MC, Johnson GE, Gray J, Fisher AJ, Corris PA, Lordan JL, Ward C. Ceramide is increased in the lower airway epithelium of people with advanced cystic fibrosis lung disease. *Am J Respir Crit Care Med* 2010; 182: 369-375.

13. Guilbault C, De Sanctis JB, Wojewodka G, Saeed Z, Lachance C, Skinner TA, Vilela RM, Kubow S, Lands LC, Hajduch M, Matouk E, Radzioch D. Fenretinide

corrects newly found ceramide deficiency in cystic fibrosis. *Am J Respir Cell Mol Biol* 2008; 38: 47-56.

14. Wojewodka G, De Sanctis JB, Radzioch D. Ceramide in cystic fibrosis: a potential new target for therapeutic intervention. *J Lipids* 2011; 2011: 674968.

15. Garic D, De Sanctis JB, Shah J, Dumut DC, Radzioch D. Biochemistry of very-long-chain and long-chain ceramides in cystic fibrosis and other diseases: The importance of side chain. *Prog Lipid Res* 2019.

16. Scholte BJ, Horati H, Veltman M, Vreeken RJ, Garratt LW, Tiddens H, Janssens HM, Stick SM, Australian Respiratory Early Surveillance Team for Cystic F. Oxidative stress and abnormal bioactive lipids in early cystic fibrosis lung disease. *J Cyst Fibros* 2019.

17. Seidl E, Kiermeier H, Liebisch G, Ballmann M, Hesse S, Paul-Buck K, Ratjen F, Rietschel E, Griese M. Lavage lipidomics signatures in children with cystic fibrosis and protracted bacterial bronchitis. *J Cyst Fibros* 2019.

18. Brodlie M, McKean MC, Johnson GE, Perry JD, Nicholson A, Verdon B, Gray MA, Dark JH, Pearson JP, Fisher AJ, Corris PA, Lordan J, Ward C. Primary bronchial epithelial cell culture from explanted cystic fibrosis lungs. *Exp Lung Res* 2010; 36: 101-110.

19. He X, Okino N, Dhami R, Dagan A, Gatt S, Schulze H, Sandhoff K, Schuchman EH. Purification and characterization of recombinant, human acid ceramidase. Catalytic reactions and interactions with acid sphingomyelinase. *J Biol Chem* 2003; 278: 32978-32986.

20. Ehlert K, Frosch M, Fehse N, Zander A, Roth J, Vormoor J. Farber disease: clinical presentation, pathogenesis and a new approach to treatment. *Pediatr Rheumatol Online J* 2007; 5: 15.

21. Li CM, Park JH, He X, Levy B, Chen F, Arai K, Adler DA, Disteche CM, Koch J, Sandhoff K, Schuchman EH. The human acid ceramidase gene (ASAH): structure, chromosomal location, mutation analysis, and expression. *Genomics* 1999; 62: 223-231.

22. He X, Dworski S, Zhu C, DeAngelis V, Solyom A, Medin JA, Simonaro CM, Schuchman EH. Enzyme replacement therapy for Farber disease: Proof-of-concept studies in cells and mice. *BBA Clin* 2017; 7: 85-96.

23. Fessler MB, Parks JS. Intracellular lipid flux and membrane microdomains as organizing principles in inflammatory cell signaling. *J Immunol* 2011; 187: 1529-1535.

24. Legler DF, Micheau O, Doucey MA, Tschopp J, Bron C. Recruitment of TNF receptor 1 to lipid rafts is essential for TNFalpha-mediated NF-kappaB activation. *Immunity* 2003; 18: 655-664.

25. Hamai H, Keyserman F, Quittell LM, Worgall TS. Defective CFTR increases synthesis and mass of sphingolipids that modulate membrane composition and lipid signaling. *J Lipid Res* 2009; 50: 1101-1108.

26. Seumois G, Fillet M, Gillet L, Faccinetto C, Desmet C, Francois C, Dewals B, Oury C, Vanderplasschen A, Lekeux P, Bureau F. De novo C16- and C24-ceramide generation contributes to spontaneous neutrophil apoptosis. *J Leukoc Biol* 2007; 81: 1477-1486.

27. Siskind LJ, Mullen TD, Romero Rosales K, Clarke CJ, Hernandez-Corbacho MJ, Edinger AL, Obeid LM. The BCL-2 protein BAK is required for long-chain ceramide generation during apoptosis. *J Biol Chem* 2010; 285: 11818-11826.

28. Cutler RG, Kelly J, Storie K, Pedersen WA, Tammara A, Hatanpaa K, Troncoso JC, Mattson MP. Involvement of oxidative stress-induced abnormalities in ceramide and cholesterol metabolism in brain aging and Alzheimer's disease. *Proc Natl Acad Sci U S A* 2004; 101: 2070-2075.

29. Kajander K, Myllyluoma E, Kyronpalo S, Rasmussen M, Sipponen P, Mattila I, Seppanen-Laakso T, Vapaatalo H, Oresic M, Korpela R. Elevated pro-inflammatory and lipotoxic mucosal lipids characterise irritable bowel syndrome. *World J Gastroenterol* 2009; 15: 6068-6074.

30. Turpin SM, Nicholls HT, Willmes DM, Mourier A, Brodesser S, Wunderlich CM, Mauer J, Xu E, Hammerschmidt P, Bronneke HS, Trifunovic A, LoSasso G, Wunderlich FT, Kornfeld JW, Bluher M, Kronke M, Bruning JC. Obesity-induced CerS6-dependent C16:0 ceramide production promotes weight gain and glucose intolerance. *Cell Metab* 2014; 20: 678-686.

31. Huang H, Kasumov T, Gatmaitan P, Heneghan HM, Kashyap SR, Schauer PR, Brethauer SA, Kirwan JP. Gastric bypass surgery reduces plasma ceramide subspecies and improves insulin sensitivity in severely obese patients. *Obesity (Silver Spring)* 2011; 19: 2235-2240.

32. Muhle C, Huttner HB, Walter S, Reichel M, Canneva F, Lewczuk P, Gulbins E, Kornhuber J. Characterization of acid sphingomyelinase activity in human cerebrospinal fluid. *PLoS One* 2013; 8: e62912.

33. Schuchman EH. Acid sphingomyelinase, cell membranes and human disease: lessons from Niemann-Pick disease. *FEBS Lett* 2010; 584: 1895-1900.

34. Callahan JW, Jones CS, Davidson DJ, Shankaran P. The active site of lysosomal sphingomyelinase: evidence for the involvement of hydrophobic and ionic groups. *J Neurosci Res* 1983; 10: 151-163.

35. Shah VS, Meyerholz DK, Tang XX, Reznikov L, Abou Alaiwa M, Ernst SE, Karp PH, Wohlford-Lenane CL, Heilmann KP, Leidinger MR, Allen PD, Zabner J, McCray PB, Ostedgaard LS, Stoltz DA, Randak CO, Welsh MJ. Airway acidification initiates host defense abnormalities in cystic fibrosis mice. *Science* 2016; 351: 503-507.

36. Schultz A, Puvvadi R, Borisov SM, Shaw NC, Klimant I, Berry LJ, Montgomery ST, Nguyen T, Kreda SM, Kicic A, Noble PB, Button B, Stick SM. Airway surface liquid pH is not acidic in children with cystic fibrosis. *Nat Commun* 2017; 8: 1409.

37. Muraglia KA, Chorghade RS, Kim BR, Tang XX, Shah VS, Grillo AS, Daniels PN, Cioffi AG, Karp PH, Zhu L, Welsh MJ, Burke MD. Small-molecule ion channels increase host defences in cystic fibrosis airway epithelia. *Nature* 2019.

38. Simonin J, Bille E, Crambert G, Noel S, Dreano E, Edwards A, Hatton A, Pranke I, Villeret B, Cottart CH, Vrel JP, Urbach V, Baatallah N, Hinzpeter A, Golec A, Touqui L, Nassif X, Galietta LJV, Planelles G, Sallenave JM, Edelman A, Sermet-Gaudelus I. Airway surface liquid acidification initiates host defense abnormalities in Cystic Fibrosis. *Sci Rep* 2019; 9: 6516.

39. Muhlebach MS, Stewart PW, Leigh MW, Noah TL. Quantitation of inflammatory responses to bacteria in young cystic fibrosis and control patients. *Am J Respir Crit Care Med* 1999; 160: 186-191.

40. Khan TZ, Wagener JS, Bost T, Martinez J, Accurso FJ, Riches DW. Early pulmonary inflammation in infants with cystic fibrosis. *Am J Respir Crit Care Med* 1995; 151: 1075-1082.

41. Armstrong DS, Grimwood K, Carlin JB, Carzino R, Gutierrez JP, Hull J, Olinsky A, Phelan EM, Robertson CF, Phelan PD. Lower airway inflammation in infants and young children with cystic fibrosis. *Am J Respir Crit Care Med* 1997; 156: 1197-1204.

42. Stoltz DA, Meyerholz DK, Pezzulo AA, Ramachandran S, Rogan MP, Davis GJ, Hanfland RA, Wohlford-Lenane C, Dohrn CL, Bartlett JA, Nelson GAt, Chang EH, Taft PJ, Ludwig PS, Estin M, Hornick EE, Launspach JL, Samuel M, Rokhlina T, Karp PH, Ostedgaard LS, Uc A, Starner TD, Horswill AR, Brogden KA, Prather RS, Richter SS, Shilyansky J, McCray PB, Jr., Zabner J, Welsh MJ. Cystic fibrosis pigs develop lung disease and exhibit defective bacterial eradication at birth. *Sci Transl Med* 2010; 2: 29ra31.

43. Sun X, Olivier AK, Liang B, Yi Y, Sui H, Evans TI, Zhang Y, Zhou W, Tyler SR, Fisher JT, Keiser NW, Liu X, Yan Z, Song Y, Goeken JA, Kinyon JM, Fligg D, Wang X, Xie W, Lynch TJ, Kaminsky PM, Stewart ZA, Pope RM, Frana T, Meyerholz DK, Parekh K, Engelhardt JF. Lung phenotype of juvenile and adult cystic fibrosis transmembrane conductance regulator-knockout ferrets. *Am J Respir Cell Mol Biol* 2014; 50: 502-512.

44. McCarron A, Donnelley M, Parsons D. Airway disease phenotypes in animal models of cystic fibrosis. *Respir Res* 2018; 19: 54.

45. Pinto SN, Silva LC, Futerman AH, Prieto M. Effect of ceramide structure on membrane biophysical properties: the role of acyl chain length and unsaturation. *Biochim Biophys Acta* 2011; 1808: 2753-2760.

46. Moore TC, Hartkamp R, Iacovella CR, Bunge AL, McCabe C. Effect of Ceramide Tail Length on the Structure of Model Stratum Corneum Lipid Bilayers. *Biophys J* 2018; 114: 113-125.

47. Abu-Arish A, Pandzic E, Kim D, Tseng HW, Wiseman PW, Hanrahan JW. Agonists that stimulate secretion promote the recruitment of CFTR into membrane lipid microdomains. *J Gen Physiol* 2019.

48. Fiedler MA, Wernke-Dollries K, Stark JM. Inhibition of TNF-alpha-induced NF-kappaB activation and IL-8 release in A549 cells with the proteasome inhibitor MG-132. *Am J Respir Cell Mol Biol* 1998; 19: 259-268.

49. Poghosyan A, Patel JK, Clifford RL, Knox AJ. Epigenetic dysregulation of interleukin 8 (CXCL8) hypersecretion in cystic fibrosis airway epithelial cells. *Biochem Biophys Res Commun* 2016; 476: 431-437.

50. Bhattacharyya S, Gutti U, Mercado J, Moore C, Pollard HB, Biswas R. MAPK signaling pathways regulate IL-8 mRNA stability and IL-8 protein expression in cystic fibrosis lung epithelial cell lines. *Am J Physiol Lung Cell Mol Physiol* 2011; 300: L81-87.

51. Floreth T, Stern E, Tu Y, Stern R, Garrity ER, Jr., Bhorade SM, White SR. Differentiated transplant derived airway epithelial cell cytokine secretion is not regulated by cyclosporine. *Respir Res* 2011; 12: 44.

52. Bonfield TL, Panuska JR, Konstan MW, Hilliard KA, Hilliard JB, Ghnaim H, Berger M. Inflammatory cytokines in cystic fibrosis lungs. *Am J Respir Crit Care Med* 1995; 152: 2111-2118.

53. Greally P, Hussein MJ, Cook AJ, Sampson AP, Piper PJ, Price JF. Sputum tumour necrosis factor-alpha and leukotriene concentrations in cystic fibrosis. *Arch Dis Child* 1993; 68: 389-392.

54. Karpati F, Hjelte FL, Wretlind B. TNF-alpha and IL-8 in consecutive sputum samples from cystic fibrosis patients during antibiotic treatment. *Scand J Infect Dis* 2000; 32: 75-79.

55. Hisert KB, Heltshe SL, Pope C, Jorth P, Wu X, Edwards RM, Radey M, Accurso FJ, Wolter DJ, Cooke G, Adam RJ, Carter S, Grogan B, Launspach JL, Donnelly SC, Gallagher CG, Bruce JE, Stoltz DA, Welsh MJ, Hoffman LR, McKone EF, Singh PK. Restoring Cystic Fibrosis Transmembrane Conductance Regulator Function Reduces Airway Bacteria and Inflammation in People with Cystic Fibrosis and Chronic Lung Infections. *Am J Respir Crit Care Med* 2017; 195: 1617-1628.

56. Schuchman EH. Acid ceramidase and the treatment of ceramide diseases: The expanding role of enzyme replacement therapy. *Biochim Biophys Acta* 2016; 1862: 1459-1471.

57. Becker KA, Riethmuller J, Seitz AP, Gardner A, Boudreau R, Kamler M, Kleuser B, Schuchman E, Caldwell CC, Edwards MJ, Grassme H, Brodlie M, Gulbins E. Sphingolipids as targets for inhalation treatment of cystic fibrosis. *Adv Drug Deliv Rev* 2018.

Figure Legends

Figure 1 – Ceramide and sphingosine levels in cystic fibrosis and non-cystic fibrosis fully differentiated primary human airway epithelial cell cultures at baseline and in response to *Pseudomonas aeruginosa*. Whole cell lysates of cystic fibrosis (CF) and non-CF cultures at baseline and after co-culture with *Pseudomonas aeruginosa* (PA), levels of total ceramide (a) and sphingosine (b). Radar charts (c) of individual ceramide species (fmole/mg protein). Plasma membrane (PM) fractions of cultures were isolated at baseline and after co-culture with *P. aeruginosa*, allowing determination of total ceramide (d) and sphingosine (e) levels. Individual ceramide species (f), displayed as radar charts (fmole/mg protein). The proportion of ceramide in plasma membranes (as a fraction of total cellular ceramide) is shown in panel (g) and equivalent for sphingosine in (h). Throughout, n=6 separate experiments from individual donors. Cultures were lysed and fractionated into whole cell and plasma membrane fractions after 28 days at air liquid interface and full differentiation. Individual data points are presented along with the mean (horizontal line) and ± standard deviation (error bars). For statistical tests used see the online data supplement *$P<0.05$, **$P<0.01$, ***$P<0.001$.

Figure 2 - Ceramide levels in BAL fluid from children and young people. Levels of ceramide in BAL fluid collected during clinically indicated bronchoscopies from children and young people with cystic fibrosis (CF) and children who do not have CF but underwent a bronchoscopy for investigation of respiratory problems. Groups were matched for age (see Table E1 in the online data supplement). Individual data points are presented along with the mean (horizontal line) and ± standard deviation (error bars). An unpaired t-test was used to determine significance *$P<0.05$.

Figure 3 – Acid ceramidase and acid sphingomyelinase expression and function in cystic fibrosis and non-cystic fibrosis airway epithelial cell cultures. (a) Apical surface activity of ceramidase (Cer), as determined by percentage of fluorescently labeled ceramide processed into sphingosine. (b) Levels of acid ceramidase (AC) protein in cystic fibrosis (CF) and non-CF cultures at baseline and after co-culture with *Pseudomonas. aeruginosa* (PA), displayed as change relative to untreated non-CF cultures. Representative blots are shown for AC, (methods for full-length blots are in the online data supplement, with details of loading controls shown in Figure E1). (c) Gene expression of *ASAH1* (coding for acid ceramidase) at baseline in CF and non-CF cultures and after co-culture with *P. aeruginosa*, displayed as fold change relative to untreated non-CF cultures. (d) Apical surface activity of sphingomyelinase (Sph), as determined by percentage of fluorescently labeled sphingomyelin processed into ceramide. (e) Levels of acid sphingomyelinase (ASM) protein, displayed as change relative to untreated non-CF cultures. Representative blots are shown for ASM (methods for full-length blots are in the online data supplement, with details of loading controls shown in Figure E1). (f) Gene expression of *SMPD1* (coding for acid sphingomyelinase), displayed as fold change relative to untreated non-CF cultures. For loading controls, antibody, and primer and reaction details see Fig E1 and Tables E2, E3 and E4 in the online data supplement. Throughout, n=6 separate experiments from individual donors. Individual data points are presented along with the mean (horizontal line) and ± standard deviation (error bars). For statistical tests used see the online data supplement *$P<0.05$, **$P\leq0.01$.

Figure 4 – Effect of recombinant human acid ceramidase treatment on ceramide and sphingosine profile of cystic fibrosis and non-cystic fibrosis airway epithelial cell cultures. Whole cell lysates of cystic fibrosis (CF) and non-CF cultures

at baseline and after treatment with recombinant human acid ceramidase (rhAC); levels of total ceramide (a) and sphingosine (b). Individual ceramide species (c), displayed as radar charts (fmol/mg protein). Plasma membrane fractions of CF and non-CF cultures at baseline and after treatment with rhAC - levels of total ceramide (d) and sphingosine (e). Individual ceramide species (f), displayed as radar charts (fmole/mg protein). Proportion of ceramide in plasma membranes (PM) (as a fraction of total cellular ceramide) is shown in panel (g) and the equivalent for sphingosine in (h). Throughout, n=6 separate experiments from individual donors. Cultures were lysed and fractionated into whole cell and plasma membrane fractions after 28 days at air liquid interface and full differentiation. Individual data points are presented along with the mean (horizontal line) and ± standard deviation (error bars). For statistical tests used see the online data supplement *P<0.05, **P≤0.01.

Figure 5 – Effect of recombinant human acid ceramidase treatment on inflammatory mediator production by cystic fibrosis and non-cystic fibrosis airway epithelial cell cultures. Time course of apical secretion of (a) IL-8, (b) IL-1β, and (c) TNFα from cystic fibrosis (CF) and non-CF cultures at baseline and after a single treatment with recombinant human acid ceramidase (rhAC). Apical secretion of IL-8 (d) from cultures following pre-treatment with combinations of ivacaftor, tezacaftor-ivacaftor and rhAC. For (a) through (c) n=6 separate experiments, n=4 for (d), CF group F508del/F508del genotype, from individual donors. Data are presented as mean with standard deviation for (a) through (c); for (d) individual data points are presented along with the mean (horizontal line) and ± standard deviation (error bars). For statistical tests used see the online data supplement *P<0.05, **P≤0.01, ***P≤0.001 and ns non-significant P≥0.05.

Figure 6 – Effect of recombinant human acid ceramidase treatment on lung inflammation in murine models. Number of (a) neutrophils and (b) macrophages in the submucosa of distal large bronchi in lung sections from wild type (WT), *Cftr^ko* and *Cftr^MHH* mice at baseline and following nebulization daily for 3 days with recombinant human acid ceramidase (rhAC). Throughout, n=6 mice in each group. Individual data points are presented along with the mean (horizontal line) and ± standard deviation (error bars). For statistical tests used see the online data supplement ***$P \leq 0.001$.

Figure 7 – Tumor Necrosis Factor Receptor 1 expression and cRel localization in cystic fibrosis airway epithelial cell cultures and lung tissue sections. Expression of Tumor Necrosis Factor Receptor 1 (TNFR1) in cystic fibrosis (CF) and non-CF cultures with and without recombinant human acid ceramidase (rhAC) treatment as assessed by (a) immunohistochemistry (with quantification of apical mean pixel intensity (MPI) in (b)). cRel expression in CF and non-CF cultures in response to *Pseudomonas aeruginosa* (PA) co-culture in the presence or absence of rhAC in (c) cytoplasmic and (d) nuclear fractions. Representative blots are shown for both (methods are in the online data supplement, with details of loading controls shown in Figure E1). (e) Apical IL-8 secretion in the presence or absence of a specific cRel inhibitor (Inh). (f) Expression and localization of cRel in airway epithelium in airway tissue sections from people with advanced CF lung disease and unused donor lungs (non-CF) with quantification of (g) whole cell and (h) nuclear localization. For (a) through (d) n=6 separate experiments, n=5 for (e) and n=4 for (f) through (h), all from individual donors, see Table S1 in the online data supplement for clinical details. Data are presented as mean with standard deviation for (b), (g) and (h); for (c) through (e) individual data points are presented along with the mean

(horizontal line) and ± standard deviation (error bars). For statistical tests used see the online data supplement *$P<0.05$, **$P\leq0.01$.
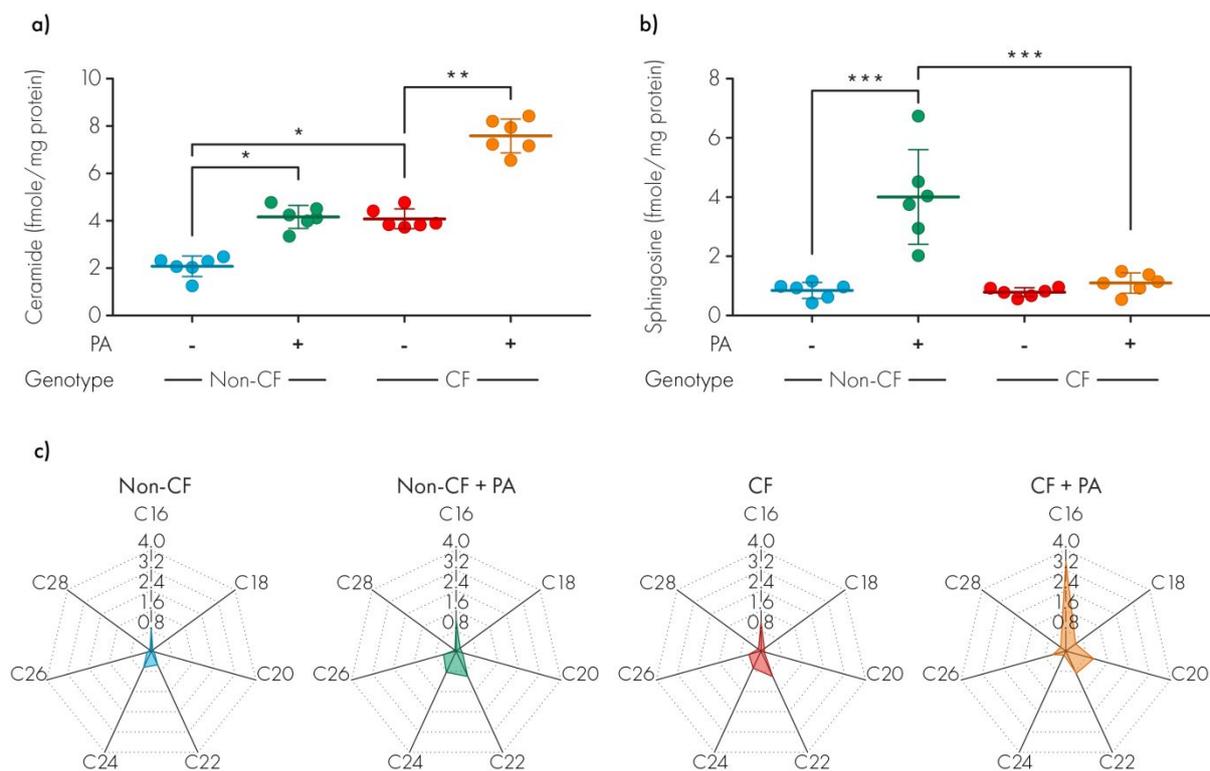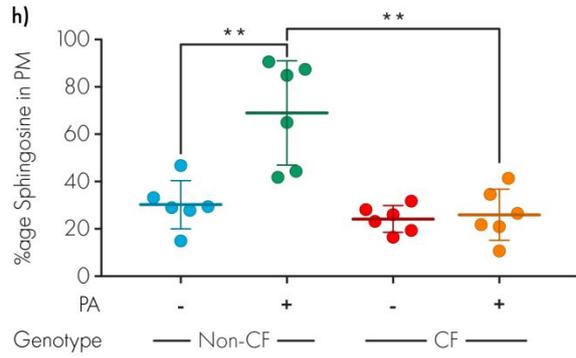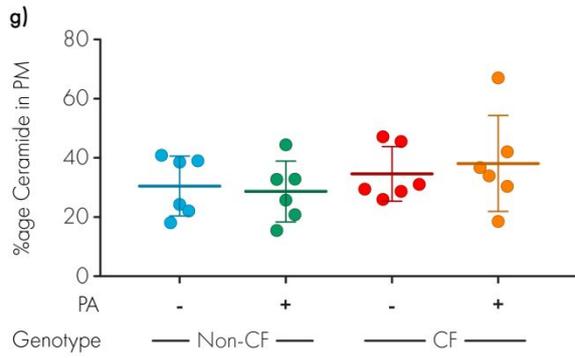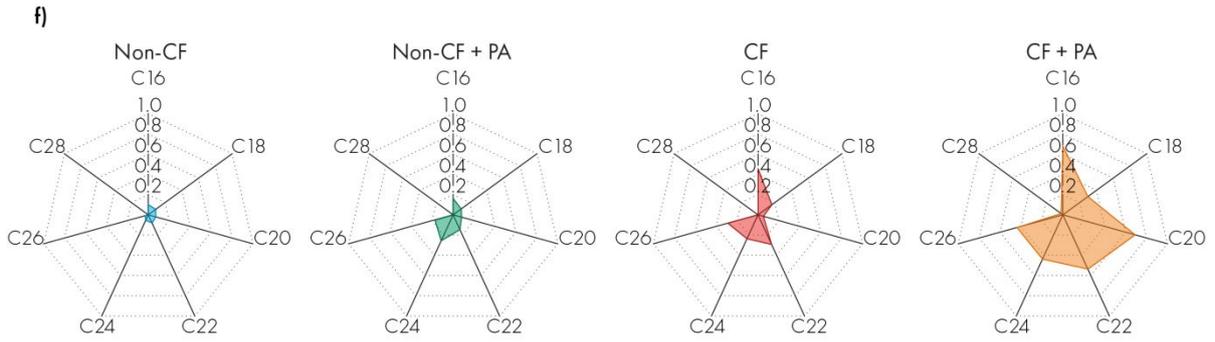
Figure 8 – Effect of recombinant human acid ceramidase treatment on infection in cystic fibrosis airway epithelial cell cultures. Number of fluorescently labeled heat-killed *Staphylococcus aureus* retrieved from apical surface washes (a), and adherent to apical surface (b) in cystic fibrosis (CF) and non-CF fully differentiated cultures with and without prior recombinant human acid ceramidase (rhAC) treatment. For representative images see Fig E6 in the online data supplement. Colony forming unit (CFU) counts of *Pseudomonas aeruginosa* isolated from (c) apical surface washes and (d) whole cell lysates (following washing, suggesting internalization) from CF and non-CF cultures with and without prior rhAC treatment. Live *P. aeruginosa* were added to the apical surface of cultures and allowed to proliferate for 24 hours. Throughout n=6 separate experiments. Individual data points are presented along with the mean (horizontal line) and ± standard deviation (error bars). For statistical tests used see the online data supplement *$P<0.05$, **$P\leq0.01$.
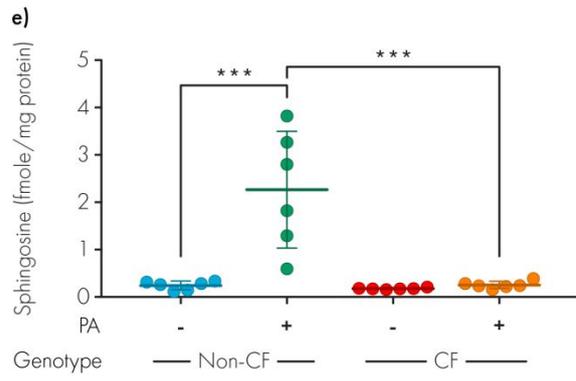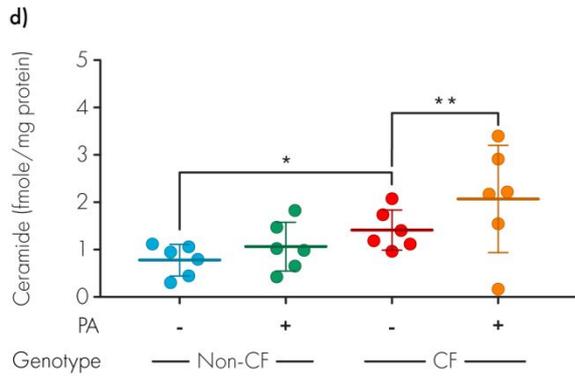
Figure 9 – Proposed model of how altered sphingolipid metabolism in cystic fibrosis airway epithelia may result in increased inflammation and susceptibility to infection. (a) In non-cystic fibrosis epithelia acid ceramidase (AC) maintains the balance of ceramide (Cer.) and sphingosine (Sph.). Normal levels of ceramide do not promote a pro-inflammatory environment and in response to *P. aeruginosa* levels of sphingosine are up-regulated. (b) In cystic fibrosis (CF) epithelia AC activity is deficient in both expression and activity which, in combination with alterations in acid sphingomyelinase activity, leads to the accumulation of ceramide. Raised ceramide is associated with increased tumor necrosis factor receptor 1 (TNFR) expression,

enhanced NF-κB activation and nuclear localization of cRel. This promotes the secretion of pro-inflammatory cytokines such as IL-8, IL-1β and TNFα. In conjunction with excessive recruitment of immune cells, which also produce pro-inflammatory mediators, a positive feedback loop emerges in the cystic fibrosis airway. Cystic fibrosis epithelia do not up-regulate sphingosine in response to *P. aeruginosa,* increasing susceptibility to infection, which further contributes to the pro-inflammatory environment. Treatment with recombinant human acid ceramidase (rhAC) reduces ceramide and increases sphingosine, ameliorating these effects.

Figures

Figure 1 – Ceramide and sphingosine levels in cystic fibrosis and non-cystic fibrosis fully differentiated primary human airway epithelial cell cultures at baseline and in response to *Pseudomonas aeruginosa*.
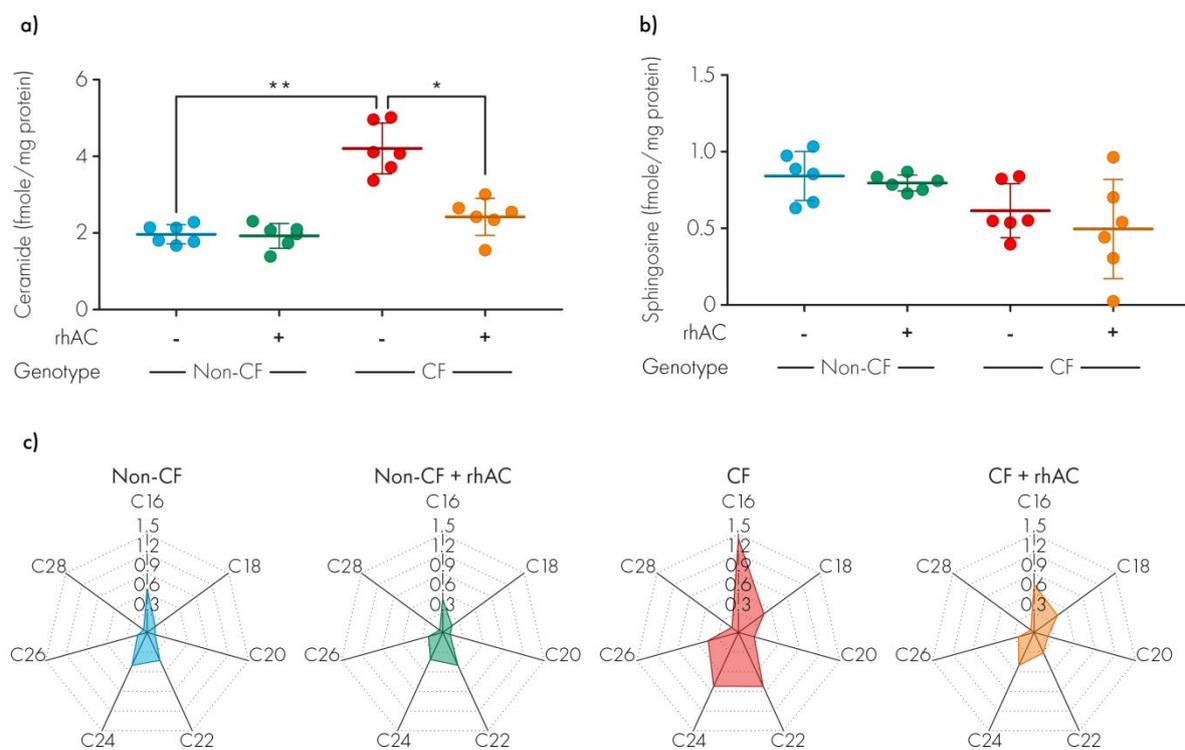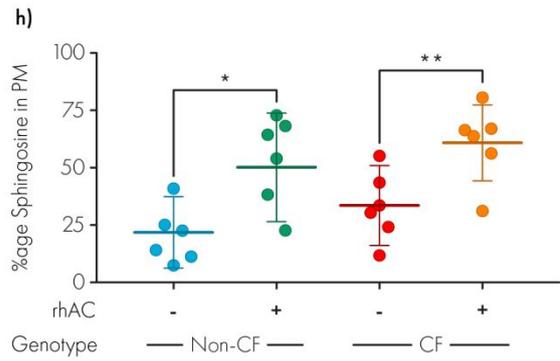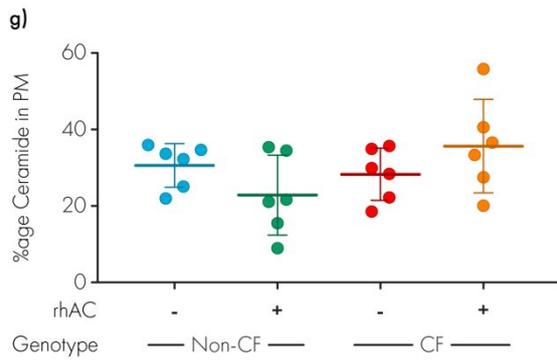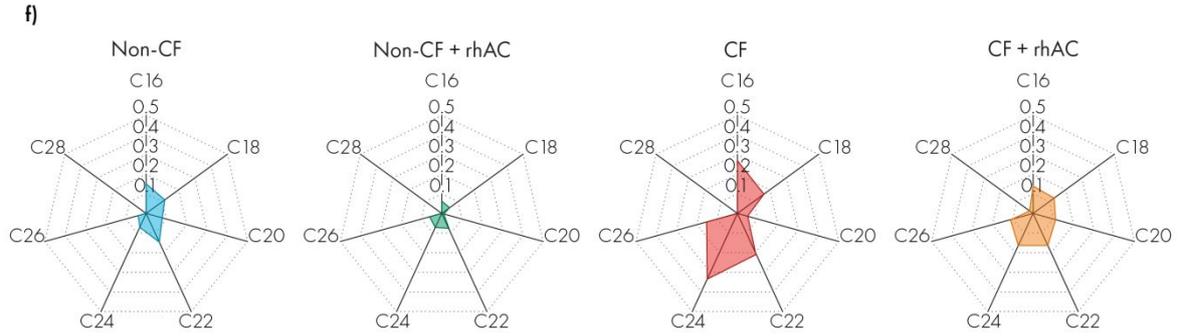
d)

e)

f)

Non-CF

Non-CF + PA

CF

CF + PA

g)

h)

Figure 2 - Ceramide levels in BAL fluid from children and young people.

a)

Figure 3 – Acid ceramidase and acid sphingomyelinase expression and function in cystic fibrosis and non-cystic fibrosis airway epithelial cell cultures.
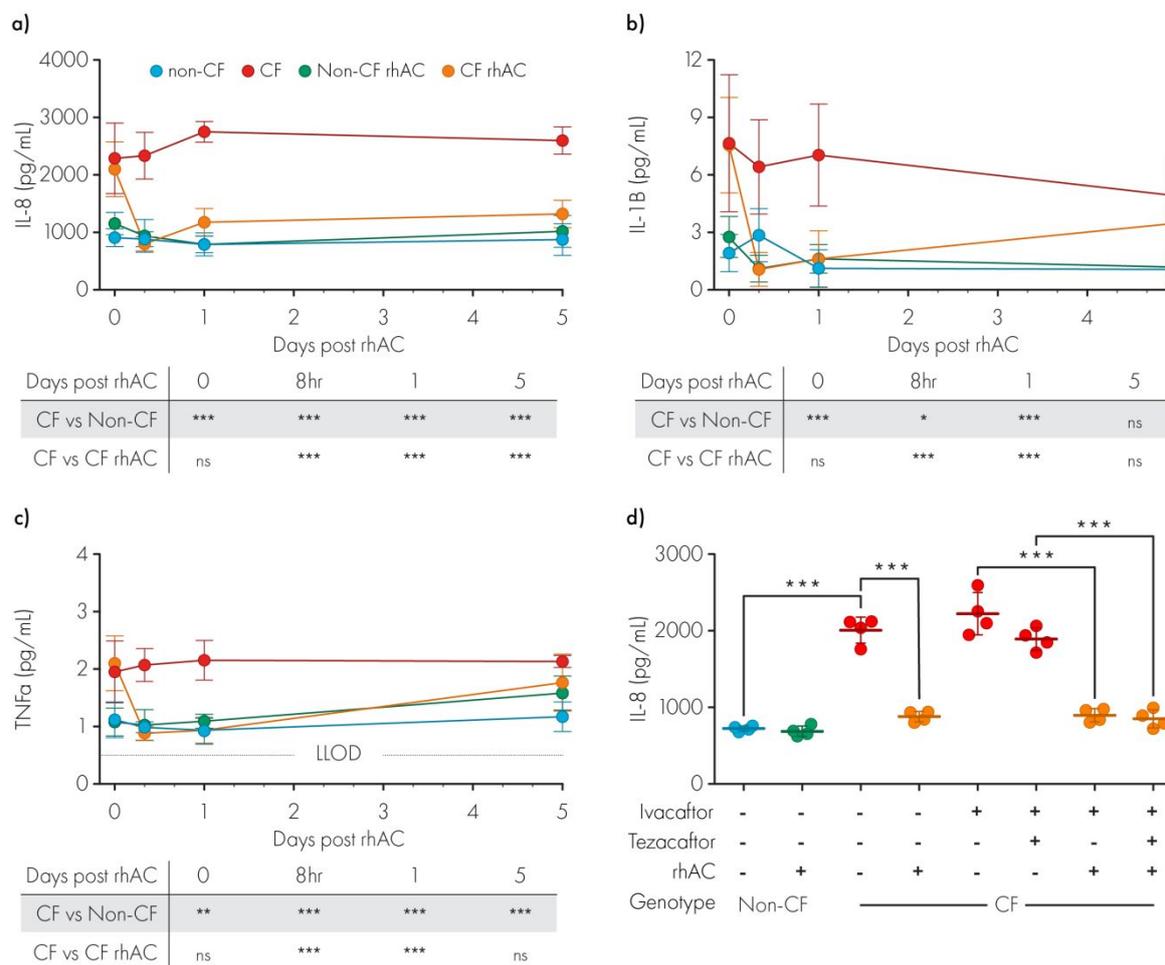
Figure 4 – Effect of recombinant human acid ceramidase treatment on ceramide and sphingosine profile of cystic fibrosis and non-cystic fibrosis airway epithelial cell cultures.
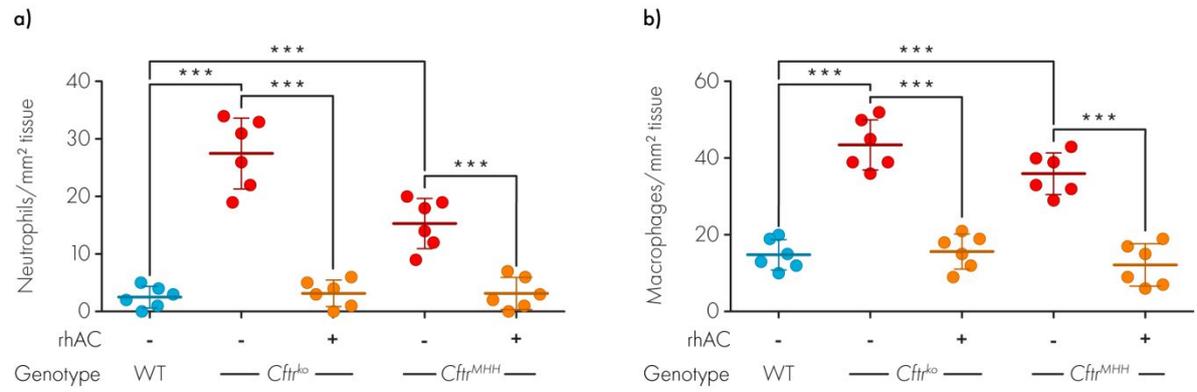
d)

e)

f)

Non-CF

Non-CF + rhAC

CF

CF + rhAC

g)

h)
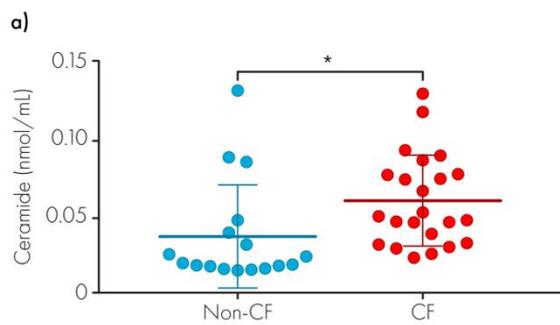
Figure 5 – Effect of recombinant human acid ceramidase treatment on inflammatory mediator production by cystic fibrosis and non-cystic fibrosis airway epithelial cell cultures.

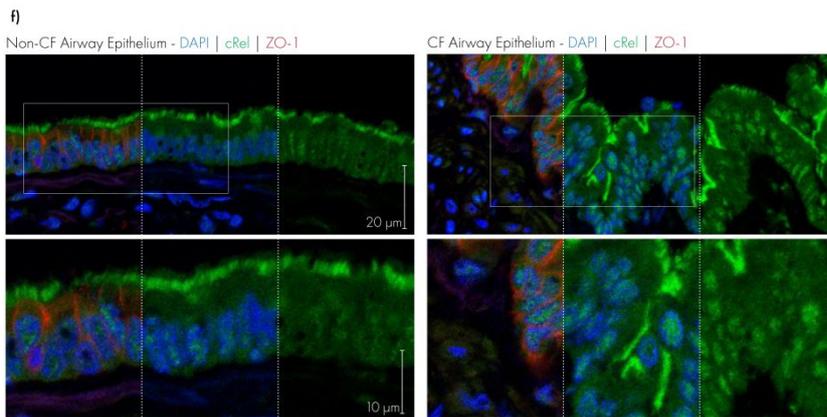**Figure 6 – Effect of recombinant human acid ceramidase treatment on lung inflammation in murine models.**

Figure 7 – Tumor Necrosis Factor Receptor 1 expression and cRel localization in cystic fibrosis airway epithelial cell cultures and tissue sections
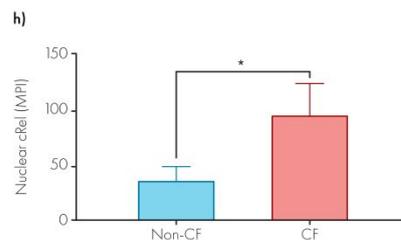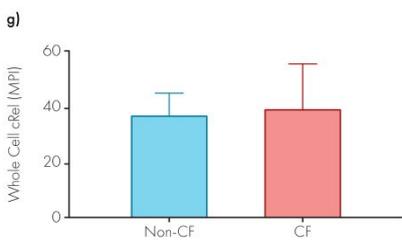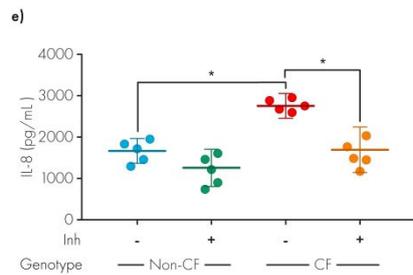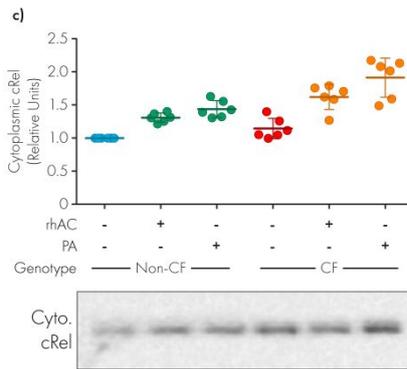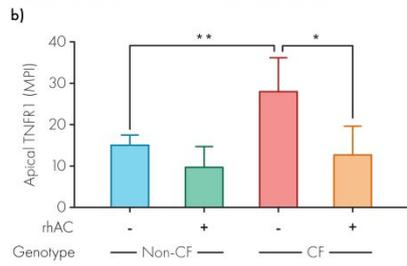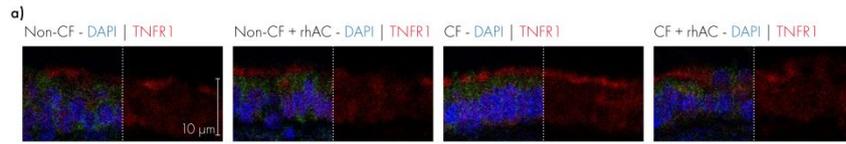
Figure 8 – Effect of recombinant human acid ceramidase treatment on infection in cystic fibrosis airway epithelial cell cultures.

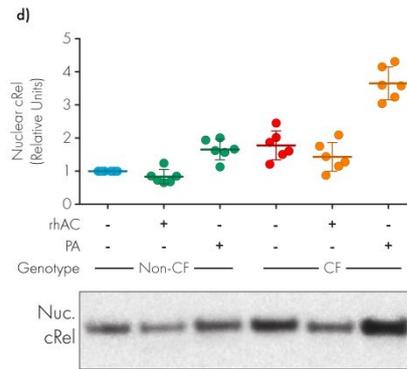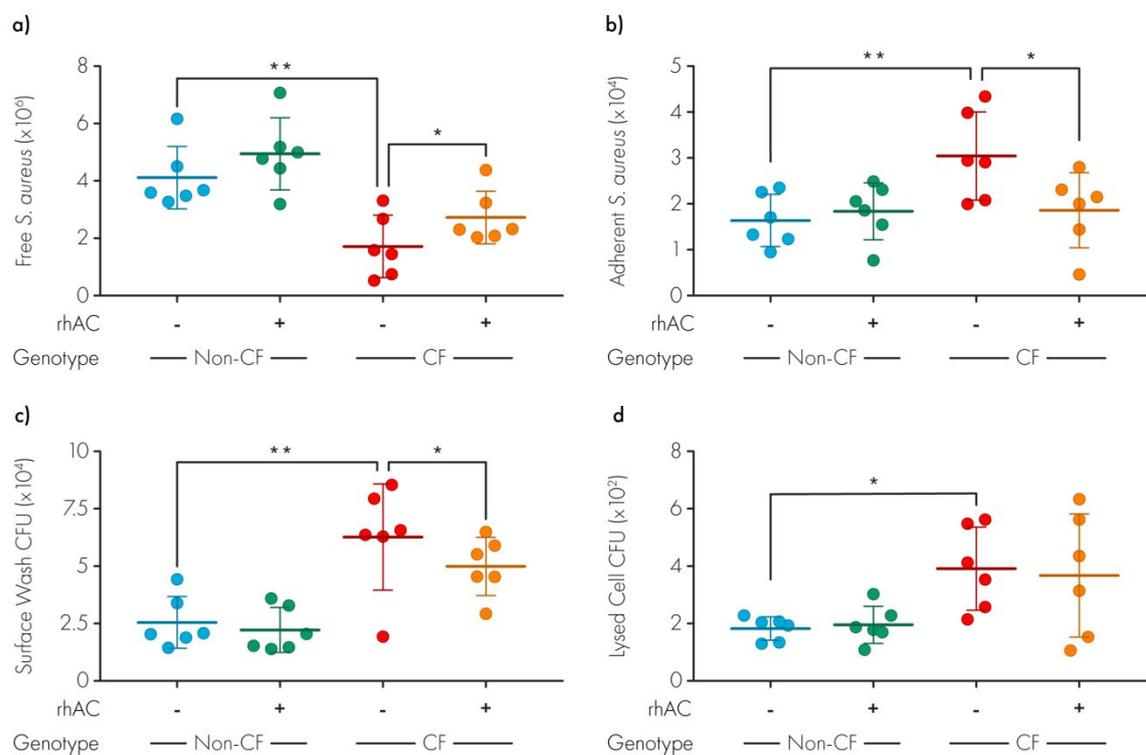**Figure 9 – Proposed model of how altered sphingolipid metabolism in cystic fibrosis airway epithelia may result in increased inflammation and susceptibility to infection.**
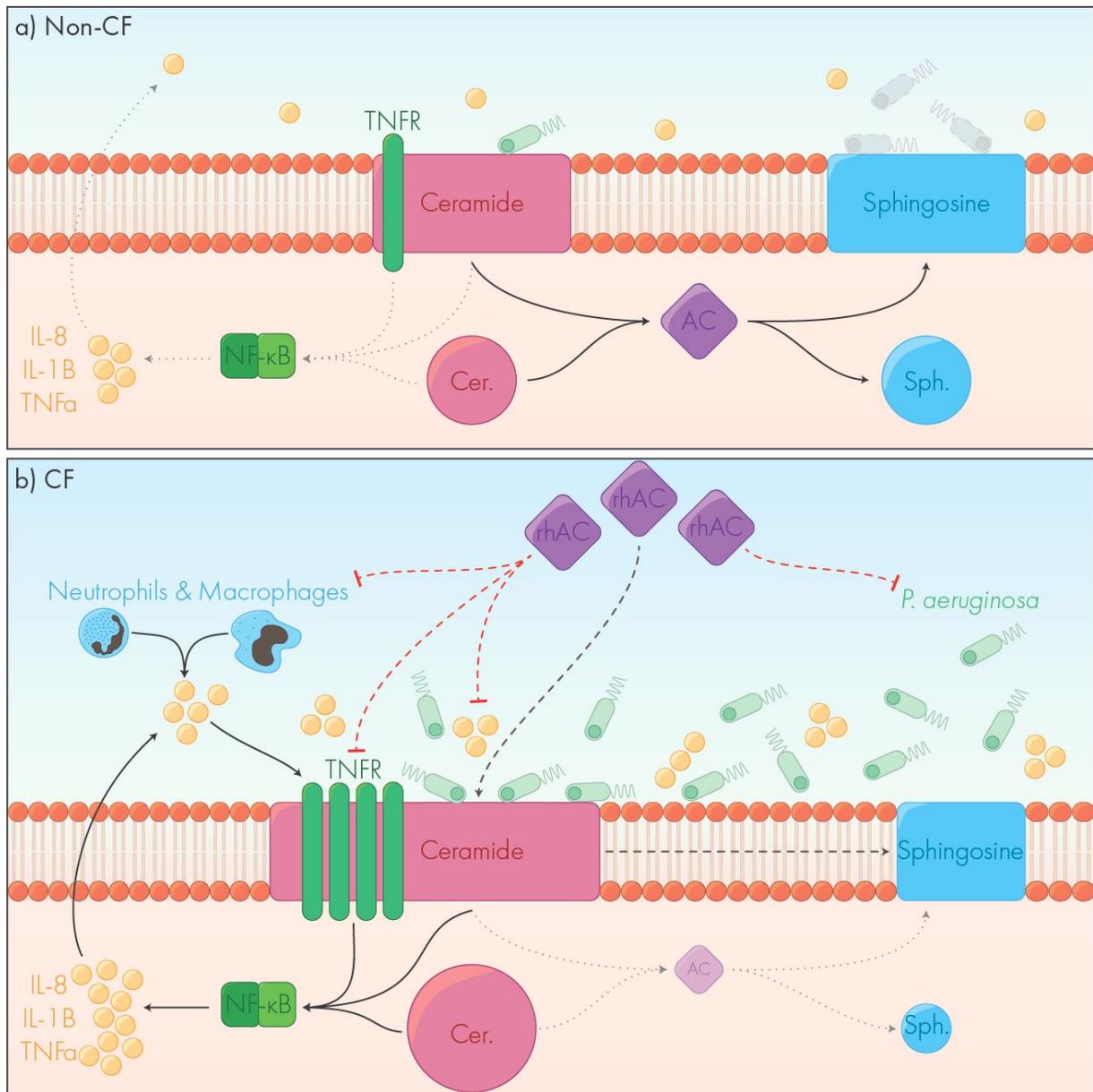
Recombinant Acid Ceramidase Reduces Inflammation and Infection in Cystic Fibrosis

Online Data Supplement

Aaron I. Gardner[1], Iram J. Haq[1,2], A. John Simpson[1], Katrin A. Becker[3], John Gallagher[1], Vinciane Saint-Criq[4], Bernard Verdon[4], Emily Mavin[1], Alexandra Trigg[1], Michael A. Gray[4], Albert Koulman[5], Melissa J. McDonnell[4,6], Andrew J. Fisher[1], Elizabeth L. Kramer[7,8], John P. Clancy[7,8], Christopher Ward[1], Edward H. Schuchman[9], Erich Gulbins[3,10] and Malcolm Brodlie*[1,2]

[1]Translational and Clinical Research Institute, Faculty of Medical Sciences, Newcastle University, Newcastle upon Tyne, UK.

[2]Paediatric Respiratory Medicine, Great North Children's Hospital, Newcastle upon Tyne Hospitals NHS Foundation Trust, Newcastle upon Tyne, UK.

[3]Respiratory Medicine, Freeman Hospital, Newcastle Upon Tyne Hospitals NHS Foundation Trust, Newcastle Upon Tyne, UK

[4]Department of Molecular Biology, University of Duisburg-Essen, Essen, Germany.

[5]Biosciences Institute, Faculty of Medical Sciences, Newcastle University, Newcastle upon Tyne, UK.

[6]NIHR BRC Metabolomics and Lipidomics Facility, University of Cambridge, Cambridge, UK.

[7]Department of Respiratory Medicine, Galway University Hospital, Galway, Ireland.

[8]Department of Pediatrics, Cincinnati Children's Hospital Medical Centre, Cincinnati, USA.

[9]Division of Pulmonary Medicine, Cincinnati Children's Hospital Medical Centre, Cincinnati, USA.

[10]Department of Genetics & Genomic Sciences, Icahn School of Medicine at Mount Sinai, New York, USA.

[11]Department of Surgery, University of Cincinnati, Cincinnati, USA.

*To whom correspondence should be addressed: Malcolm Brodlie, MRC Clinician Scientist/Honorary Consultant in Paediatric Respiratory Medicine, Level 3, Clinical Resource Building, Great North Children's Hospital, Queen Victoria Road, Newcastle upon Tyne, UK, NE1 4LP. E-mail: malcolm.brodlie@ncl.ac.uk. Tel: +44 191 2336161.

Supplementary methods

Primary airway epithelial cell culture and patient demographics

Primary bronchial epithelial cells (PBECs) were isolated from the explanted native lungs of people with CF, undergoing lung transplantation. All people with CF had 2 disease-causing *CFTR* variants and had developed severe CF lung disease leading to transplantation. Patient demographics for the CF and non-CF groups are provided in Table E1. Non-CF PBECs were sampled from main bronchi via bronchoscopic brushings from 3 adults with non-CF bronchiectasis, 1 unused donor lung and 2 lobectomy specimens for distal lung cancer.

PBECs were expanded as submerged monolayer cultures, prior to differentiation as air liquid interface (ALI) cultures, as previously described[1]. All cultures generated cilia, produced mucus and had a trans-epithelial resistance >250 $\Omega*cm^2$.

Pseudomonas aeruginosa and airway epithelial cell co-cultures

One day prior to assay, ALI cultures were transitioned to completely antibiotic and serum-free medium, and washed apically. Single colonies of freshly plated *P. aeruginosa* (PA01) (ATCC) were inoculated in 10 mL of LB broth (Thermo Fisher Scientific, Waltham, MA, USA) and grown overnight at 37 °C under agitation. Optical density at 600 nM was determined and $1x10^5$ colony forming units (CFU) in 100 µL phosphate-buffered saline (PBS) were added to the apical surface of ALI cultures, and incubated for 24 hours.

Recombinant human acid ceramidase treatment of epithelial cell cultures

ALI cultures were prepared as above prior to treatment apically with 100 µL of rhAC (generated as described previously[2]) at a concentration of 20 µg/mL for 1 hour under

1

standard conditions. Residual liquid was then removed and cultures then either analyzed or used for ongoing culture.

Modulator treatment of epithelial cell cultures

ALI cultures treated basolaterally with either 5 µM ivacaftor or 5 µM ivacaftor and 5 µM tezacaftor (both Selleck Chemicals Houston, TX, USA), for 48 hours, with the dose replenished after 24 hours.

cRel inhibitor treatment

ALI cultures were prepared as above prior to treatment basolaterally with the highly selective and potent cRel inhibitor IT 901 (Tocris, Bristol, UK) at a final concentration of 2 µM for 24 hours under standard conditions(3).

Sample preparation

For lipid analysis

Lipids were isolated by the Folch method(4). Briefly, ALI cultures were scraped into 500 µL ice cold PBS and agitated. 10 µL was removed for BCA protein assay (Thermo Fisher Scientific), to allow for normalization, and the remainder pelleted at 5,000 x g. The pellet was resuspended in chloroform:methanol (2:1 v/v) (Sigma-Aldrich, Gillingham, UK) and gently mixed for 5 minutes. A half volume of de-ionized water was added and the sample centrifuged at 250 x g for 5 minutes to separate the phases. The lower phase was removed and evaporated at room temperature and stored at -80 °C prior to analysis. Plasma membrane fractions were isolated following a graded ultracentrifugation process.

2

For Western blotting

ALI cultures were scraped into 1 mL of ice cold RIPA buffer containing a protease inhibitor cocktail (Roche, Basel, Switzerland). Where required nuclear and cytoplasmic fractions were generated using the NE-PER extraction kit (Thermo Fisher Scientific). Samples were vortexed for 30 seconds before being briefly sonicated. Protein concentration was determined by BCA protein assay and samples stored at -80 °C prior to analysis.

For Real-time qPCR

ALI cultures were scraped into 500 μL ice cold PBS before being pelleted at 5,000 x g. Samples were then processed as per the Purelink RNA Micro Kit manufacturer's instructions (Thermo Fisher Scientific). RNA concentration and quality were determined using a NanoDrop One. Standard concentrations of cDNA were generated using random hexamer primers.

For cytokine quantification assay

The apical surface of cultures was washed three times with 100 μL of PBS before starting the experiment. At each timepoint the apical surface of cultures was incubated with 100 μL of PBS for 5 minutes. The fluid was aspirated and stored at -80 °C prior to analysis. 250 μL of basal media was also collected at each timepoint and replaced with fresh medium.

3

For immunohistochemistry

Patient tissue (clinical details are in Table E1) or ALI cultures were fixed in 4% paraformaldehyde before being dehydrated and embedded in paraffin for sequential transverse sectioning. Sections were dewaxed and rehydrated through sequential washes (Xylenes, 100%, 95%, 70%, 50% ethanol, cold tap water). Antigen retrieval consisted of boiling for 1 minute in 10 mM sodium citrate buffer. This was performed on tissue but not ALI sections.

Mass spectrometry

Calibration curves for all assayed ceramide and sphingosine species were constructed using appropriate standards (Avanti Polar Lipids, Alabaster, AL, USA). All standards and samples were analyzed in triplicate with the ABSciex QTrap 4000 system, using a 3-scan event methodology to reduce matrix noise. For selectivity the mass tolerance for each ion was set to within 0.01 m/z, which allowed for accurate quantification.

Bronchoalveolar lavage sampling and ceramide measurement

Following informed consent bronchoalveolar lavage fluid was sampled from 23 children and young people with CF (median age 8.7 years, range 0.2 to 20.8 years) and from 17 children and young people without CF (median age 8.5 years, range 0.7 to 15.2 years) but with respiratory problems undergoing clinically-indicated bronchoscopies. The physician performing the bronchoscopy determined the location of sample collection and the volume of instilled sterile saline, typically 1 to 3 instillations of 10 mL aliquots(5). Clinical characteristics are provided in Table E1. Both groups were matched for age.

4

Cell-free supernatant samples of bronchoalveolar lavage fluid were analyzed. For ceramide determination, a ceramide hydrolysis buffer (0.2 M citric/phosphate buffer, pH 4.5 containing 0.3 M NaCl and 0.2 mg/ml of recombinant acid ceramidase) was mixed with the total lipid extract solution (1:1,v/v) and incubated at 37 °C for 60 min. This mixture was then incubated for an additional 10 min at 50 °C with a fluorogenic reaction buffer (25 mM sodium borate buffer, pH 9) containing 1.25 mM sodium cyanide and 1.25 mM naphthalene-2,3-dicarboxyaldehyde (NDA) to derivatize the ceramide hydrolysis product, sphingosine. The mixture was then centrifuged (13,000 × g for 10 minutes) and the supernatant was analyzed using an Acquity H-Class UPLC system (Waters, Milford, MA, USA) equipped with a Waters Acquity UPLC BEH RP18 column (2.0 × 50 mm, 1.7 μm). The fluorescent (NDA) sphingosine was monitored at excitation and emission wavelengths of 252 and 483 nm, respectively. Quantification of the sphingosine peak was calculated using the Waters Empower software according to a standard curve derived from commercial (Invitrogen) NDA sphingosine.

Ceramidase and sphingomyelinase functional *in situ* assays

A derivation of the previously described fluorescent ceramidase and sphingomyelinase assays was utilized to determine enzyme activity[6]. Briefly, 100 μL of buffered solution containing either BODIPY® TR Ceramide or BODIPY® FL C12-Sphingomyelin (both Thermo Fisher Scientific) at a 1:2000 dilution was applied to the apical surface of ALI cultures. After one hour of incubation residual liquid was removed and a further 2 x 100 μL PBS washes performed. The lipid fraction was isolated as described above and samples were separated by thin layer chromatography with chloroform:methanol (5:1 v/v), then analyzed on a Typhoon fluorescence plate reader.

5

Western blotting

20 µg of whole cell lysates, 10 µg of cytoplasmic fraction, or 6 µg of nuclear fraction, isolated as described above, were separated by SDS-PAGE and transferred to PVDF membranes (BioRad). Membranes were blocked for 1 hour with 3% BSA in PBS-Tween (Sigma) before being probed with appropriate primary and isotype-matched HRP-conjugated secondary antibodies (Table E2). Membranes were then treated with SuperSignal West PICO plus chemiluminescent substrate (Thermo Fisher Scientific) and exposed to film. Membranes were stripped and re-probed for β-actin as a loading control, and exposed. Films were scanned and samples normalized against their respective loading controls.

Real-time qPCR

Relative gene expression was determined by real-time qPCR. 1 ng of previously standardized cDNA per sample (in duplicate) was analyzed using the primers and conditions described (Tables E3 & E4) on a QuantStudio 3 system. "Template only" and "negative only" controls were performed as required, and genes of interest were normalized against combined *GAPDH, ACTB* and *TUBB*.

Cytokine quantification

Apical washes, and basal medium samples, were taken from CF and non-CF cultures which had been treated with rhAC at 0-, 8-, 24- and 120-hour intervals. Samples were analyzed using a custom Meso Scale Discovery U-PLEX assay (IL-1β, IL-4, IL-6, IL-8 and TNFα; MSD, Rockville, MD, USA), or DuoSet ELISA kit (IL-8 and TNFα; R&D Systems, Minneapolis, MN, USA) as per the manufacturer's instructions. Where

6

appropriate the lower limit of detection (LLOD) is displayed on the graph (any values below this threshold were excluded from statistical analysis).

Mice

Two different *Cftr* mutant mouse strains and their respective syngeneic littermates were used. *Cftr^{tm1Unc}-Tg$^{(FABPCFTR)}$* (abbreviated *Cftr^{KO}*) Jaw mice (Jackson Laboratories, Bar Harbor, ME, US) are genetically deficient for the murine equivalent to human CFTR (*Cftr*), but express human CFTR in the gut under control of a fatty acid binding protein promoter to prevent acute intestinal obstruction[7, 8]. The mice were backcrossed for more than 20 generations on a C57BL/6 background. B6.129P2(CF/3)-*Cftr$^{TgH(neoim)Hgu}$* (abbreviated *Cftr^{MHH}*) congenic mice were used as previously described[9, 10]. These mice have a low residual activity of Cftr allowing normal development and feeding. Mice were housed in isolator cages in a pathogen-free environment. The hygienic status was repeatedly tested by a panel of common murine pathogens according to the FELASA recommendations of 2002[11].

Nebulization of recombinant human acid ceramidase

Cftr^{KO} mice were nebulized with rhAC 200 µg diluted in 800 µL 0.9% NaCl solution using Pari boy nebulizer apparatus (PARI, Starnberg, Germany) over 10 minutes. rhAC was nebulized on 3 consecutive days between 08:00 and 09:00 when mice were 24 weeks old. The trachea was removed 6 hours after the last inhalation and immediately snap frozen in liquid nitrogen.

Determination of neutrophil and macrophage numbers in murine lung tissues

Cryostat thin sections (5 µm) were prepared from lung tissues, fixed on glass slides with acetone, washed with PBS-2% Tween, blocked with normal goat serum (1:10

7

diluted in PBS-0.2% Tween), washed and incubated overnight at 4°C with monoclonal antibodies to murine neutrophils or to macrophages in PBS-0.5% Triton. Sections were washed with PBS-0.1% Tween and incubated with Cy2-labeled goat anti-mouse antibodies (Table E2) for 1 h at room temperature, washed 3-times with PBS-0.1% Tween and incubated with 2 µg/ml of 4,6-diamidino-2-phenylindole-dihydrochloride (DAPI; Boehringer, Mannheim, Germany) in PBS-0.1% Tween at room temperature, to allow discrimination of neutrophils and macrophages. The sections were washed and embedded with Mowiol®. For quantitative determination of cell numbers, five sections per mouse lung were examined and relevant cells were evaluated in the submucosa of distal large bronchi. The observer was blinded. From every section, 6 to 10 digitalized images were taken. Sections were analyzed with a Leica DMIRE2.

Immunohistochemistry

Slides were washed for 5 minutes in PBS plus 0.1% Triton X-100, twice, before being blocked with a 1% BSA solution in PBS-0.5% Tween for one hour at room temperature. Samples were incubated with primary antibodies (Table E2) overnight at 4 °C. Slides were washed three times for 5 minutes in PBS Tween before incubation with appropriate fluorescently conjugated secondary antibodies (Table E2) for 2 hours. Slides were washed three times for 5 minutes in PBS Tween before being incubated with DAPI as a nuclear counterstain for 5 minutes. Samples were then mounted in Mowiol® mounting media and coverslips were added. All images were acquired on a Nikon A1 confocal microscope. Appropriate blank and secondary only controls were performed as required.

8

Staphylococcus aureus adherence assay

100 μL of a 10,000 particles/mL solution of heat-killed, fluorescently labeled *S. aureus* particles (Sigma) were added to the apical surface of ALI cultures and incubated for 1 hour. Residual liquid was gently removed and *S. aureus* particles counted. Simultaneously, cultures were fixed in 4% PFA before being counterstained with DAPI (Sigma-Aldrich). Membranes were removed, mounted in Mowiol® mounting media and cover slips were applied. Images were acquired using a Zeiss Axioimager and counts performed with the observer blinded.

Pseudomonas aeruginosa adherence and internalization assay

P. aeruginosa-epithelial co-cultures were prepared as described above. Following rhAC treatment, 1×10^5 CFU in 100 μL of PBS were added to the apical surface of ALI cultures, and incubated for 24 hours. The apical surface of the cultures was robustly washed three times with 100 μL of PBS, and serial dilutions of the final wash were plated out for determination of adherent CFU. ALI cultures were then lysed and plated out to assess bacterial internalization.

Statistics

Mass spectrometry measurements of sphingolipids

Individual data points are presented along with the mean (horizontal line) and ± standard deviation (error bars). Statistical significance was determined using an unpaired t-test or one-way ANOVA with multiple comparisons (Tukey corrected) where appropriate. The proportion of each sphingolipid, in the plasma membrane, relative to the total amount for each sample was also calculated. Data are shown as individual points and are presented along with the mean (horizontal line) and ± standard

9

deviation (error bars). Statistical significance was determined using a Kruskal-Wallis test with Dunn's multiple comparisons.

Ceramidase and sphingomyelinase functional assays

Individual data points are presented along with the mean (horizontal line) and ± standard deviation (error bars). Statistical significance was determined using an unpaired t-test.

Real-time qPCR

Data are presented as fold change ($2-\Delta\Delta Ct$) relative to untreated non-CF samples. Statistical significance was determined using an unpaired t-test.

Cytokine quantification

Data are presented as the mean and ± standard deviation (error bars). Statistical significance was determined using a two-way ANOVA with multiple comparisons (Tukey corrected).

Mouse immune cell counts and cytokine quantification

Individual data points are presented along with the mean (horizontal line) and ± standard deviation (error bars). Statistical significance was determined using a two-way ANOVA with multiple comparisons (Tukey corrected).

Immunohistochemistry Mean Pixel Intensity (MPI)

Individual data points are presented along with the mean (horizontal line) and ± standard deviation (error bars). Statistical significance was determined using either an unpaired t-test or one-way ANOVA with multiple comparisons (Tukey corrected).

10

Staphylococcus adherence assay

Individual data points are presented along with the mean (horizontal line) and ± standard deviation (error bars). Statistical significance was determined using a one-way ANOVA with multiple comparisons (Tukey corrected).

Pseudomonas aeruginosa adherence and internalization assay

Individual data points are presented along with the mean (horizontal line) and ± standard deviation (error bars). Statistical significance was determined using a one-way ANOVA with multiple comparisons (Tukey corrected).

Cell viability assays

Cells were treated with various doses of recombinant human acid ceramidase (rhAC) for 24 hours. Both the Presto Blue™ (Thermo Fisher Scientific) viability assay and lactate dehydrogenase cytotoxicity (Thermo Fisher Scientific) assay were performed as per manufacturer's instructions.

Ceramide quantification in mouse trachea

Mice were inhaled as described in the methods section. The trachea was removed after treatment, shock frozen in liquid nitrogen, homogenized in 200 µl H_2O by 3 cycles of sonication using a tip sonicator and extracted in 600 µl $CHCl_3:CH_3OH:1N$ HCl (100:100:1, v/v/v). The lower phase was dried, resuspended in 20 µL of a detergent solution (7.5% [w/v] n-octyl glucopyranoside, 5 mM cardiolipin in 1 mM diethylenetriaminepentaacetic acid [DTPA]), and 70 µl of 0.01 units diacylglycerol (DAG) kinase (Biomol, Germany) in 0.1 M imidazole/HCl (pH 6.6), 0.2 mM DTPA (pH 6.6), 70 mM NaCl, 17 mM $MgCl_2$, 1.4 mM ethylene glycol tetra acetic acid; 1 µM ATP and 10 µCi [32P] ATP were added. The samples were incubated for 30 min at 37^oC

11

with shaking (350 rpm) and processed as above. The kinase reaction was terminated by addition of 1 mL CHCl3:CH3OH:1N HCl (100:100:1, v/v/v) followed by addition of 170 µL buffered saline solution (135 m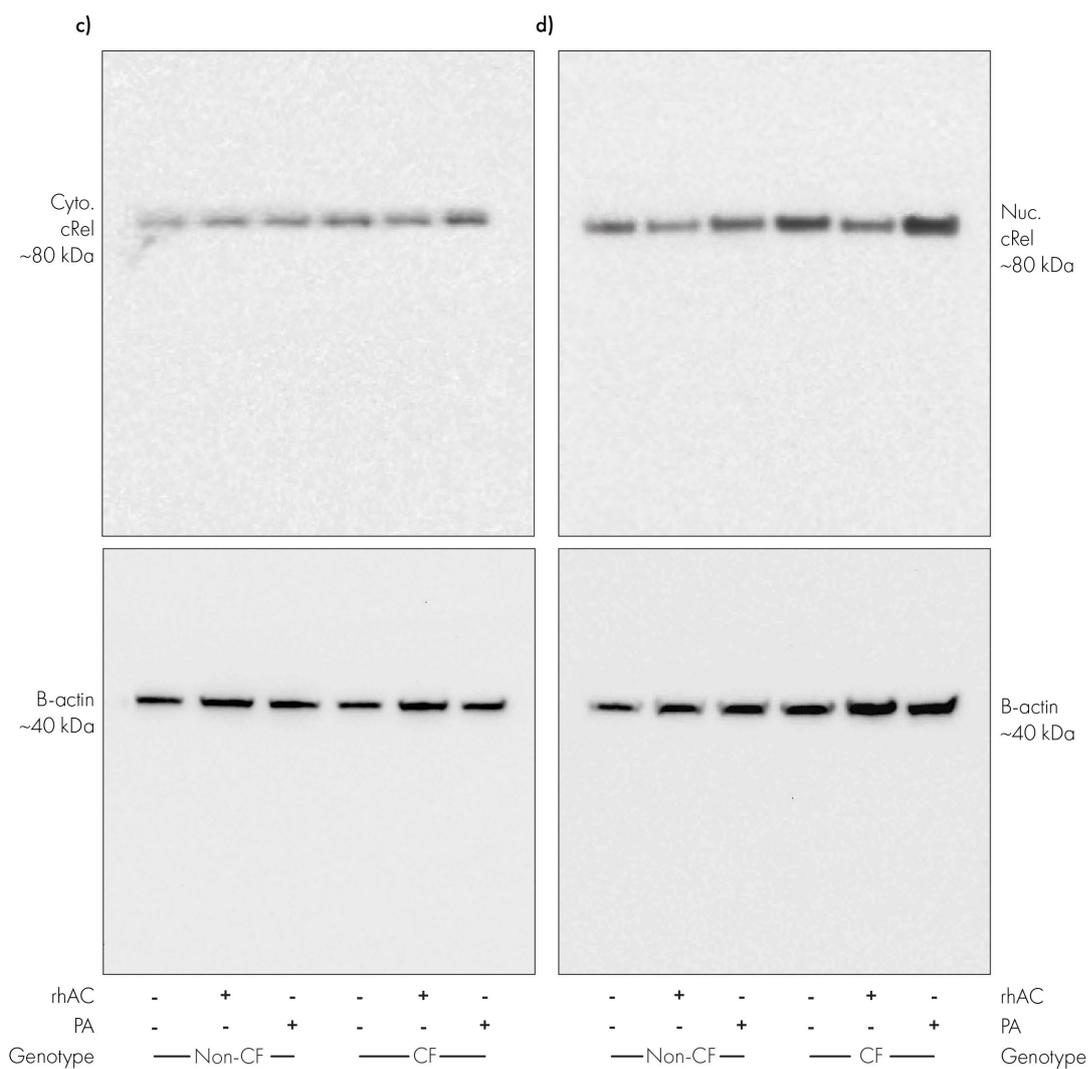M NaCl, 1.5 mM CaCl2, 0.5 mM MgCl2, 5.6 mM glucose, 10 mM HEPES, pH 7.2) and 30 µL of a 100 mM EDTA solution were added. Phases were separated, the lower phase was collected, dried, dissolved in 20 µL of CHCl3:CH3OH (1:1, v/v) and separated on Silica G60 thin-layer chromatography (TLC) plates using CHCl3/acetone/CH3OH/acetic acid/H2O (50:20:15:10:5, v/v/v/v/v). The TLC plates were analyzed employing a phospho-imager. Ceramide was determined by comparison with a standard curve of C16- to C24-ceramides.

Study approvals

Written informed consent was received from participants prior to inclusion. The use of tissue and cells was approved by Local Research Ethics Committees (Newcastle and North Tyneside, reference 11/NE/029 and Galway University Hospitals, reference C.A.771). Bronchoalveolar lavage sampling was approved by the Cincinnati Children's Hospital Medical Center Institutional Review Board. All procedures performed on mice were approved by the Animal Care and Use Committee of the Bezirksregierung Duesseldorf, Duesseldorf, Germany.

12

Supplementary figures

a)

b)

AC
~50 kDa

ASM
~70 kDa

B-actin
~40 kDa

B-actin
~40 kDa

| PA | - | + | - | + |
| Genotype | Non-CF | | CF | |

| - | + | - | + | PA |
| Non-CF | | CF | | Genotype |

13

c)

d)

Cyto.
cRel
~80 kDa

Nuc.
cRel
~80 kDa

B-actin
~40 kDa

B-actin
~40 kDa

rhAC	-	+	-	-	+	-		-	+	-	-	+	-	rhAC
PA	-	-	+	-	-	+		-	-	+	-	-	+	PA
Genotype	——Non-CF ——			——CF——				——Non-CF—			—— CF ——			Genotype
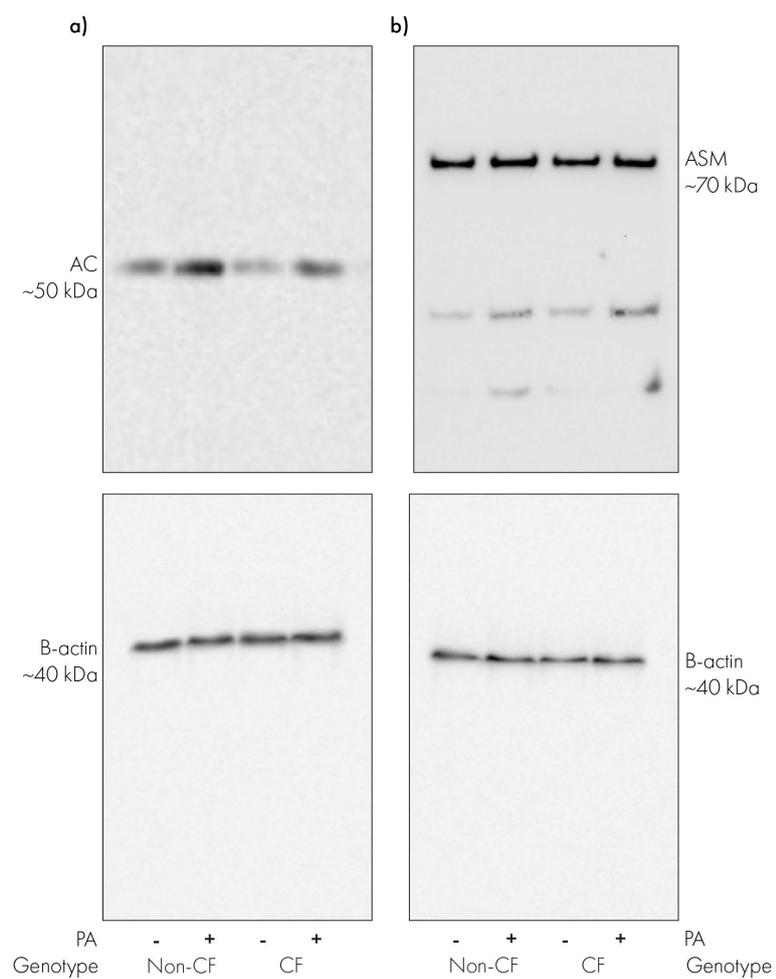
Figure E1 – Representative full-length Western blots and loading controls for acid ceramidase, acid sphingomyelinase and cRel expression in cystic fibrosis and non-cystic fibrosis epithelial cell cultures from the main manuscript. Corresponding to Figs 3b, 3e, 7c and 7d in the main manuscript. Representative full-length Western blots for acid ceramidase (AC) (a), acid sphingomyelinase (ASM) (b), cytoplasmic cRel (c) and nuclear cRel (d), with associated β-actin loading controls from the same membrane.

14
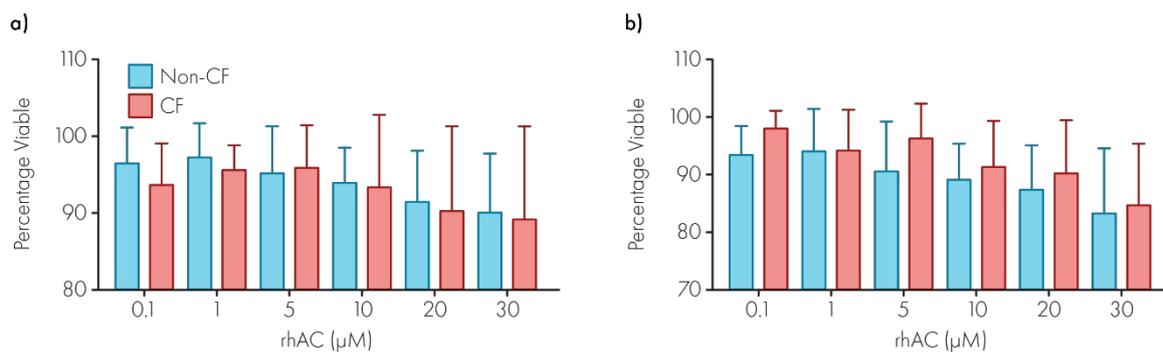
Figure E2 – Recombinant human acid ceramidase toxicity studies in airway epithelial cells. Effect of differing concentrations of recombinant human acid ceramidase (rhAC) on cell viability of cystic fibrosis (CF) and non-CF airway epithelial cell cultures measured by (a) Presto Blue™ viability assay and (b) lactate dehydrogenase cytotoxicity assay. Throughout, n=5 individual donors. Data are presented as mean with standard deviation. For statistical tests used see methods. No significant differences detected.

15
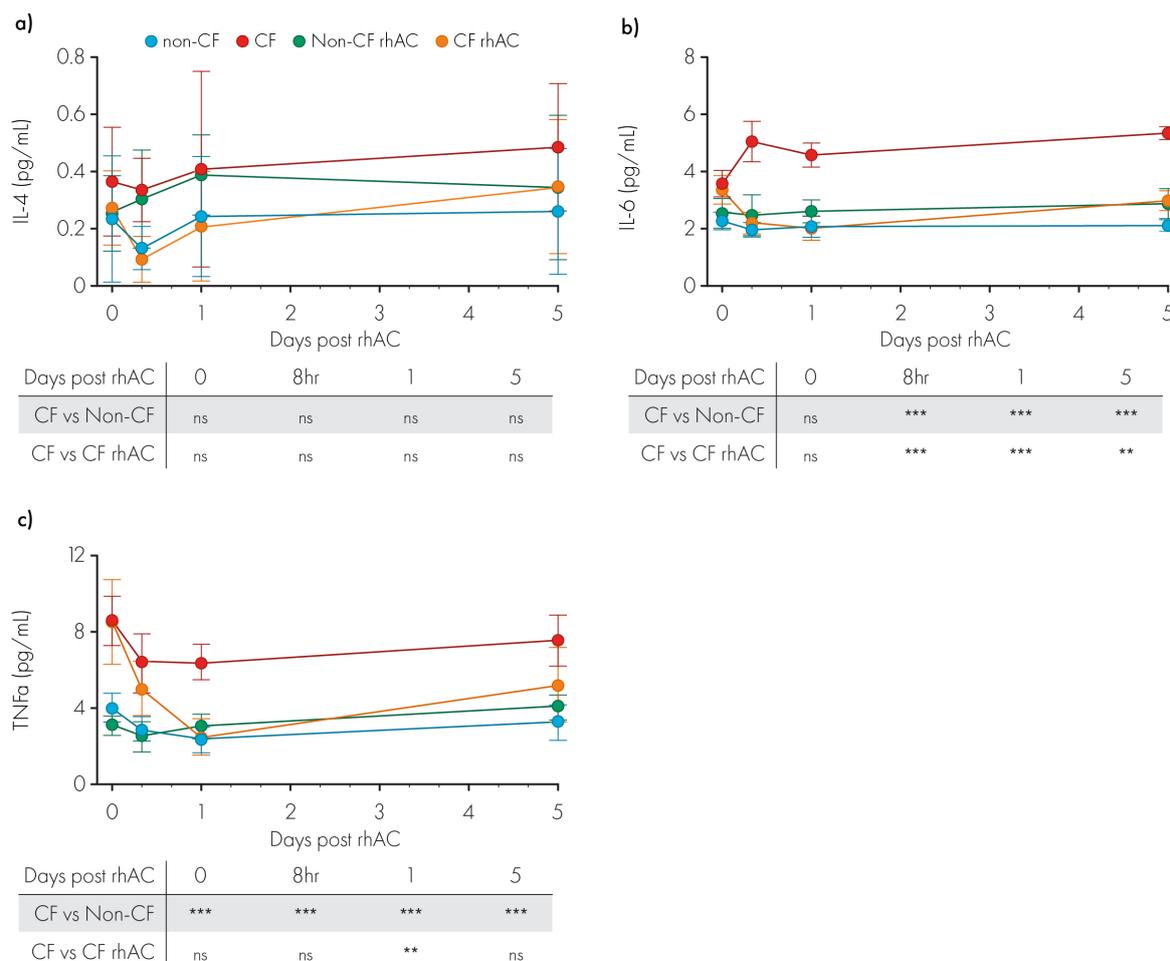
Figure E3 - Effect of recombinant human acid ceramidase treatment on inflammatory mediator production by cystic fibrosis and non-cystic fibrosis airway epithelial cell cultures (other cytokines and chemokines not shown in Figure 5). The apical surface of cystic fibrosis (CF) and non-CF airway epithelial cell cultures was washed with 100 µL sterile phosphate buffered saline. Cultures were then apically treated with recombinant human acid ceramidase (rhAC) and additional washes performed at 8-, 24- and 120-hours post-treatment (a) IL-4 and (b) IL-6 apical secretion time course. (c) TNFα measured in the basolateral medium over the same experiments. LLOD refers to lower limit of detection for assay used. Throughout n=6 individual donors. Data presented as mean with standard deviation. For statistical tests used see methods **$P \le 0.01$, ***$P \le 0.001$ and ns non-significant $P \ge 0.05$.

16
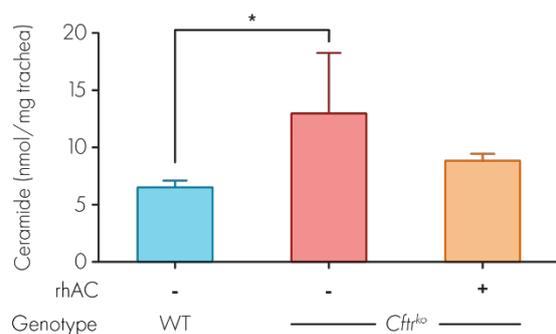
Figure E4 – Effect of recombinant human acid ceramidase treatment on ceramide concentration in the trachea of mice. (a) Concentration of ceramide in the trachea of wild type (WT) and *Cftr*^{KO} mice at baseline and following daily nebulization for 3 days of recombinant human acid ceramidase (rhAC). Throughout, n=4 mice. Data presented as mean with standard deviation. For statistical tests used see methods *P<0.05.

17

a)
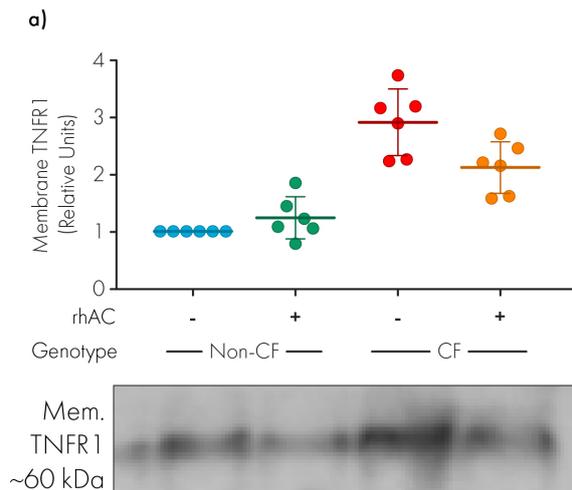
Figure E5 – Western blotting of Tumor Necrosis Factor Receptor 1 in the plasma membrane of cystic fibrosis and non-cystic fibrosis airway epithelial cell cultures. Representative Western blot and quantification of Tumor Necrosis Factor Receptor 1 (TNFR1) present in the plasma membrane fraction of cystic fibrosis (CF) and non-CF airway epithelial cultures. Membrane fractions from standardized whole cell lysates were separated through the use of ultracentrifugation prior to Western blotting. Samples were standardized against a non-CF control as no reliable housekeeping marker could be determined for the plasma membrane fraction. Throughout n=6 individual donors. Individual data points are presented along with the mean (horizontal line) and ± standard deviation (error bars).

18

a)   b)
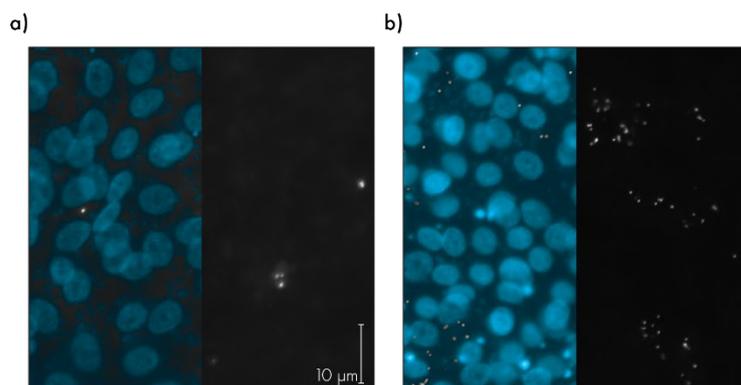
Figure E6 – Representative images of *Staphylococcus aureus* particles adherent to the surface of non-cystic fibrosis and cystic fibrosis airway epithelial cell cultures. Representative images of fluorescently labeled *Staphylococcus aureus* adherent to the surface of (a) non-cystic fibrosis (CF) and (b) CF fully differentiated airway epithelial cell cultures. Fluorescent particles are visible as white dots in the merge (left) and without DAPI (right) panels.

19

Supplementary tables

Table E1 – Demographics of patients sampled in the study

Diagnosis	*CFTR* genotype	Age (years)	Sex
Demographics of people sampled for primary airway epithelial cell culture (Figures 1,3,4,5,7,8)			
Cystic fibrosis	p.Phe508del / p.Arg560Thr	43	Male
	p.Phe508del / p.Phe508del	41	Male
	p.Phe508del / p.Phe508del	30	Male
	p.Phe508del / p.Phe508del	36	Male
	p.Phe508del / p.Phe508del	28	Female
	p.Phe508del / p.Gly542Ter	32	Male
Non-CF bronchiectasis	*Not applicable*	34	Female
Non-CF bronchiectasis		47	Female
Non-CF bronchiectasis		34	Male
Unused donor lung		28	Male
Lobectomy		44	Female
Lobectomy		48	Male
Demographics of children and young people from whom bronchoalveolar lavage fluid was sampled (Figure 2)			
Cystic fibrosis	Not recorded	18	Female
	p.Phe508del / p.Phe508del	3	Female
	p.Phe508del / p.Leu206Trp	2 months	Female
	p.Phe508del / p.Phe508del	3 months	Male
	p.Phe508del / p.Phe508del	1	Male
	p.Phe508del / p.Phe508del	4	Female
	c.1022_1023insTC / Unknown	5	Male
	p.Phe508del / p.Phe508del	7	Female
	p.Phe508del / p.Phe508del	16	Male
	p.Phe508del / p.Phe508del	7	Female
	p.Phe508del / p.Phe508del	6	Male
	p.Phe508del / c.3272-76A>G	16	Female
	p.Phe508del / c.489+1G>T	10	Female
	Not recorded	13	Female
	p.Phe508del / p.Phe508del	12	Female
	Not recorded	17	Male
	p.Phe508del / p.Phe508del	8	Female
	Not recorded	15	Male
	p.Phe508del / p.Phe508del	11	Female
	p.Phe508del / p.Phe508del	6	Male
	p.Phe508del / p.Phe508del	3	Male
	Not recorded	15	Female
	Not recorded	20	Male
Upper airway obstruction	*Not applicable*	8 months	Male
Tracheomalacia		1	Male
Not recorded		2	Male
Subglottic stenosis		3	Male
Subglottic stenosis		3	Male

20

Diagnosis	*CFTR* genotype	Age (years)	Sex
Subglottic stenosis, bronchiectasis	*Not applicable*	3	Female
Tracheomalacia		6	Male
Adenotonsillar hypertrophy		6	Male
Upper airway obstruction		8	Female
Bronchiectasis		9	Female
Recurrent pneumonia		11	Female
Upper airway obstruction		13	Female
Not recorded		13	Male
Subglottic stenosis, bronchiectasis		15	Male
Not recorded		15	Female
Upper airway obstruction, bronchiectasis		17	Male
Tracheal stenosis		18	Male
Demographics of patients sampled for immunohistochemistry of lung tissue (Figure 7)			
Cystic fibrosis	p.Phe508del / p.Phe508del	41	Male
	p.Phe508del / p.Phe508del	30	Male
	p.Phe508del / p.Phe508del	36	Male
	p.Phe508del / p.Phe508del	28	Female
Unused donor lung	*Not applicable*	52	Female
Unused donor lung		61	Female
Unused donor lung		52	Female
Unused donor lung		64	Male

Table E2 – Antibody details

Target	Host (isotype)	Supplier	Catalogue number
Acid ceramidase	Rabbit (IgG)	Mybiosource	MBS1492517
Acid sphingomyelinase	Mouse (IgG)	Abcam	ab74281
CD68	Mouse (IgG1)	Acris	AM50195PU
TNFR1	Rabbit (IgG)	Abcam	ab19139
cRel	Rabbit (IgG)	Cell Signaling	4727S
Actin	Mouse (IgG2a)	Sigma	A2228
Cy2 conjugated anti mouse	Goat	Abcam	ab6944
HRP conjugated anti mouse	Goat	ThermoFisher Scientific	31430
HRP conjugated anti rabbit	Goat	ThermoFisher Scientific	31460
AF488 conjugated anti mouse	Goat	ThermoFisher Scientific	A-11001
AF488 conjugated anti rabbit	Goat	ThermoFisher Scientific	A-11008
AF594 conjugated anti mouse	Goat	ThermoFisher Scientific	A-11005
AF594 conjugated anti rabbit	Goat	ThermoFisher Scientific	A-11012

21

Table E3 – qPCR reaction details

	UDG activation	Denature	Denature	Anneal/Extend	
Temperature	50 °C	95 °C	95 °C	60 °C	
Time	2 min	10 min	15 sec	1 min	

Table E4 – qPCR primer details

Gene	Forward Primer	Reverse Primer
ASAH1	ACCAGTGCCTGGCCTACTT	AACAGCGGCAATACCCTTCA
SMPD1	GAAGGGAAAAGAAAGAATTGGGGG	GAGAGAGATGAGGCGGAGAC
GAPDH	GTCTCCTCTGACTTCAA	ACCACCCTGTTGCTGTA
ACTB	TGAGAGGGAAATCGTGCGTG	TGCTTGCTGATCCACATCTGC
TUBB	ACTACCAGCCACCCTCTGTGTC	GCACAAACGCACGATTACA

22

Supplementary references

E1. Brodlie M, McKean MC, Johnson GE, Perry JD, Nicholson A, Verdon B, Gray MA, Dark JH, Pearson JP, Fisher AJ, Corris PA, Lordan J, Ward C. Primary bronchial epithelial cell culture from explanted cystic fibrosis lungs. *Exp Lung Res* 2010; 36: 101-110.

E2. He X, Okino N, Dhami R, Dagan A, Gatt S, Schulze H, Sandhoff K, Schuchman EH. Purification and characterization of recombinant, human acid ceramidase. Catalytic reactions and interactions with acid sphingomyelinase. *J Biol Chem* 2003; 278: 32978-32986.

E3. Shono Y, Tuckett AZ, Liou HC, Doubrovina E, Derenzini E, Ouk S, Tsai JJ, Smith OM, Levy ER, Kreines FM, Ziegler CG, Scallion MI, Doubrovin M, Heller G, Younes A, O'Reilly RJ, van den Brink MR, Zakrzewski JL. Characterization of a c-Rel Inhibitor That Mediates Anticancer Properties in Hematologic Malignancies by Blocking NF-kappaB-Controlled Oxidative Stress Responses. *Cancer Res* 2016; 76: 377-389.

E4. Folch J, Lees M, Sloane Stanley GH. A simple method for the isolation and purification of total lipides from animal tissues. *J Biol Chem* 1957; 226: 497-509.

E5. Noah TL, Black HR, Cheng PW, Wood RE, Leigh MW. Nasal and bronchoalveolar lavage fluid cytokines in early cystic fibrosis. *J Infect Dis* 1997; 175: 638-647.

E6. Grassme H, Henry B, Ziobro R, Becker KA, Riethmuller J, Gardner A, Seitz AP, Steinmann J, Lang S, Ward C, Schuchman EH, Caldwell CC, Kamler M, Edwards MJ, Brodlie M, Gulbins E. beta1-Integrin Accumulates in Cystic Fibrosis Luminal Airway Epithelial Membranes and Decreases Sphingosine, Promoting Bacterial Infections. *Cell Host Microbe* 2017; 21: 707-718 e708.

23

E7. Snouwaert JN, Brigman KK, Latour AM, Malouf NN, Boucher RC, Smithies O, Koller BH. An animal model for cystic fibrosis made by gene targeting. *Science* 1992; 257: 1083-1088.

E8. Zhou L, Dey CR, Wert SE, DuVall MD, Frizzell RA, Whitsett JA. Correction of lethal intestinal defect in a mouse model of cystic fibrosis by human CFTR. *Science* 1994; 266: 1705-1708.

E9. Teichgraber V, Ulrich M, Endlich N, Riethmuller J, Wilker B, De Oliveira-Munding CC, van Heeckeren AM, Barr ML, von Kurthy G, Schmid KW, Weller M, Tummler B, Lang F, Grassme H, Doring G, Gulbins E. Ceramide accumulation mediates inflammation, cell death and infection susceptibility in cystic fibrosis. *Nat Med* 2008; 14: 382-391.

E10. Dorin JR, Dickinson P, Alton EW, Smith SN, Geddes DM, Stevenson BJ, Kimber WL, Fleming S, Clarke AR, Hooper ML, et al. Cystic fibrosis in the mouse by targeted insertional mutagenesis. *Nature* 1992; 359: 211-215.

E11. Nicklas W, Baneux P, Boot R, Decelle T, Deeny AA, Fumanelli M, Illgen-Wilcke B, Felasa. Recommendations for the health monitoring of rodent and rabbit colonies in breeding and experimental units. *Lab Anim* 2002; 36: 20-42.

24